

## CRITICAL REVIEW

---

# INTENSITY-MODULATED RADIOTHERAPY: CURRENT STATUS AND ISSUES OF INTEREST

Intensity Modulated Radiation Therapy Collaborative Working Group

## TABLE OF CONTENTS

### ABSTRACT

*IMRT treatment plan test cases*

### INTRODUCTION

*QA checks of monitor unit calculations*

*IMRT treatment verification*

*Recommendations: Acceptance testing, commissioning, and*

*QA of IMRT systems and treatment verification*

### IMRT HISTORICAL REVIEW

*3D treatment planning systems*

*Precursors to IMRT delivery systems*

### FACILITY PLANNING AND RADIATION SAFETY

*Workload estimates*

*Dose rate and calibration changes*

*Shielding design*

*Patient whole-body dose*

*Recommendations: Facility planning and radiation safety*

### IMRT DELIVERY TECHNIQUES

*Scanned photon and electron beam IMRT*

*Tomotherapy IMRT*

*Conventional multileaf collimator IMRT*

*Physical modulator (compensating filter) IMRT*

*Robotic linear accelerator IMRT*

### TARGET VOLUME AND DOSE SPECIFICATION AND REPORTING

*Target volume specification*

*Dose specification*

*Recommendations: Target volume and dose specification*

### COMPUTER OPTIMIZATION

*Objective functions*

*Computer optimization (search) process*

*Leaf sequence generation*

### CLINICAL EXPERIENCE

### DOSE DISTRIBUTION AND MONITOR UNIT CALCULATIONS FOR IMRT

*Calculation algorithm types*

*Important issues for IMRT dose calculations*

*Monitor unit calculations for IMRT*

*Recommendations: IMRT dose calculations*

### SUMMARY AND CONCLUSIONS

### ACKNOWLEDGMENTS

### IMRT ACCEPTANCE TESTING, COMMISSIONING, AND QA

*Acceptance testing of the IMRT treatment planning system*

*Verification of IMRT dose distributions*

### APPENDIX A: IMRT NOMENCLATURE

### REFERENCES

Intensity Modulated Radiation Therapy Collaborative Working Group: Arthur L. Boyer, Ph.D., E. Brian Butler, M.D., Thomas A. DiPetrillo, M.D., Mark J. Engler, Ph.D., Benedick Fraass, Ph.D., Walter Grant, III, Ph.D., C. Clifton Ling, Ph.D., Daniel A. Low, Ph.D., Thomas R. Mackie, Ph.D., Radhe Mohan, Ph.D., James A.

Purdy, Ph.D. (Chairman), Mack Roach, M.D., Julian G. Rosenman, M.D., Ph.D., Lynn J. Verhey, Ph.D., and John W. Wong, Ph.D. National Cancer Institute: Richard L. Cumberlin, M.D., Helen Stone, Ph.D. American Association of Physicists in Medicine Liaison: Jatinder R. Palta, Ph.D.

**Purpose.** To develop and disseminate a report aimed primarily at practicing radiation oncology physicians and medical physicists that describes the current state-of-the-art of intensity-modulated radiotherapy (IMRT). Those areas needing further research and development are identified by category and recommendations are given, which should also be of interest to IMRT equipment manufacturers and research funding agencies.

**Methods and Materials.** The National Cancer Institute formed a Collaborative Working Group of experts in IMRT to develop consensus guidelines and recommendations for implementation of IMRT and for further research through a critical analysis of the published data supplemented by clinical experience. A glossary of the words and phrases currently used in IMRT is given in the Appendix. Recommendations for new terminology are given where clarification is needed.

**Results.** IMRT, an advanced form of external beam irradiation, is a type of three-dimensional conformal radiotherapy (3D-CRT). It represents one of the most important technical advances in RT since the advent of the medical linear accelerator. 3D-CRT/IMRT is not just an add-on to the current radiation oncology process; it represents a radical change in practice, particularly for the radiation oncologist. For example, 3D-CRT/IMRT requires the use of 3D treatment planning capabilities, such as defining target volumes and organs at risk in three dimensions by drawing contours on cross-sectional images (i.e., CT, MRI) on a slice-by-slice basis as opposed to drawing beam portals on a simulator radiograph. In addition, IMRT requires that the physician clearly and quantitatively define the treatment objectives. Currently, most IMRT approaches will increase the time and effort required by physicians, medical physicists, dosimetrists, and radiation therapists, because IMRT planning and delivery systems are not yet robust enough to provide totally automated solutions for all disease sites. Considerable research is needed to model the clinical outcomes to allow truly automated solutions. Current IMRT delivery systems are essentially first-generation systems, and no single method stands out as the ultimate technique. The instrumentation and methods used for IMRT quality assurance procedures and testing are not yet well established. In addition, many fundamental questions regarding IMRT are still unanswered. For example, the radiobiologic consequences of altered time–dose fractionation are not completely understood. Also, because there may be a much greater ability to trade off dose heterogeneity in the target vs. avoidance of normal critical structures with IMRT compared with traditional RT techniques, conventional radiation oncology planning principles are challenged. All in all, this new process of planning and treatment delivery has significant potential for improving the therapeutic ratio and reducing toxicity. Also, although inefficient currently, it is expected that IMRT, when fully developed, will improve the overall efficiency with which external beam RT can be planned and delivered, and thus will potentially lower costs.

**Conclusion.** Recommendations in the areas pertinent to IMRT, including dose–calculation algorithms, acceptance testing, commissioning and quality assurance, facility planning and radiation safety, and target volume and dose specification, are presented. Several of the areas in which future research and development are needed are also indicated. These broad recommendations are intended to be both technical and advisory in nature, but the ultimate responsibility for clinical decisions pertaining to the implementation and use of IMRT rests with the radiation oncologist and radiation oncology physicist. This is an evolving field, and modifications of these recommendations are expected as new technology and data become available. © 2001 Elsevier Science Inc.

IMRT, 3D treatment planning, Inverse planning, Optimization, Dose calculations, 3D conformal therapy, Quality assurance.

## INTRODUCTION

Radiotherapy (RT) planning and delivery are in the process of changing dramatically. This change is being driven in large part by continuing advances in computer hardware and software that has led to the development of sophisticated three-dimensional radiation treatment planning (3D-RTP) and computer-controlled radiation therapy (CCRT) delivery systems (1–3). Such planning and delivery systems have made practical the implementation of three-dimensional conformal radiation therapy (3D-CRT). The goal of 3D-CRT is to conform the spatial distribution of the prescribed dose to the 3D target volume (cancerous cells plus a margin for spatial uncertainties) and at the same time minimize the dose to the surrounding normal structures. Typically, the delivery of

3D-CRT is accomplished with a set of fixed radiation beams, which are shaped using the projection of the target volume. The radiation beams normally have a uniform intensity across the field, or, where appropriate, have this intensity modified by simple beam fluence-modifying devices, such as wedges or compensating filters.

However, even before this form of 3D-CRT (henceforth referred to as *conventional 3D-CRT*) has been implemented throughout the radiation oncology community, a new type of conformal planning and delivery technology is evolving. This new type of 3D-CRT, *intensity-modulated radiation therapy* (IMRT), is based on the use of optimized non-uniform radiation beam intensities incident on the patient (Fig. 1) (4, 5). IMRT treatment plans are often generated using *inverse planning* or *automated optimization* 3D-RTP

Reprint requests to: James A. Purdy, Ph.D., Radiation Oncology Center, Mallinckrodt Institute of Radiology, 510 South Kingshighway Blvd., St. Louis, MO 63110.

**Acknowledgments**—The IMRT CWG thanks the members of the Radiation Therapy Committee of the American Association of Physicists in Medicine chaired by Jatinder Palta and the members

of the Medical Physics Committee of the American Society for Therapeutic Radiology and Oncology chaired by Randall Ten Haken for their review and helpful suggestions.

Received Oct 24, 2000, and in revised form Jul 3, 2001. Accepted for publication Jul 6, 2001.

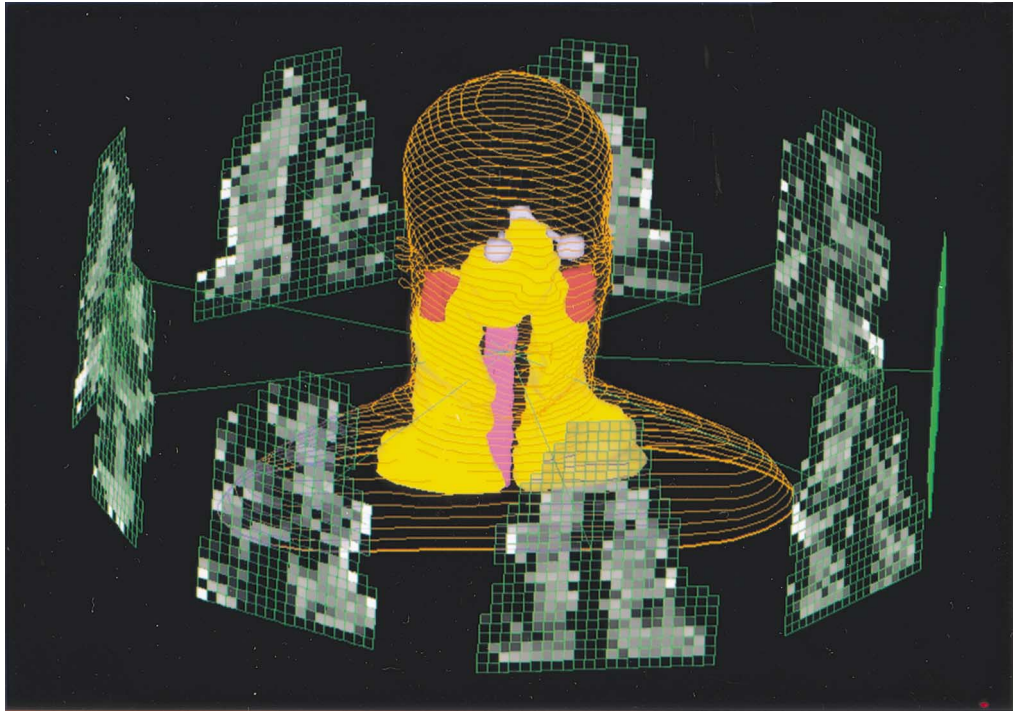


Fig. 1. Advanced form of 3D-CRT—IMRT—which is based on the use of optimized non-uniform radiation beam intensities incident on the patient. Shown is a 3D view of the patient, the PTV, spinal cord, and parotid glands, and the 9 intensity modulated beams (with gray levels reflecting the intensity value) used to generate the IMRT dose distribution.

systems, which use computer optimization techniques to help determine the distribution of intensities across the target volume.

In any new area of technology, new words and new uses of old words rapidly come into being. Although this is necessary and desirable, a poorly defined term can lead to a misunderstanding in reporting the clinical results and also in research and development. For example, various other descriptors have been used in the past in reference to IMRT, including generalized 3D-CRT, unconstrained 3D-CRT, and computer-controlled conformal RT (2, 4, 6–9). The IMRT Collaborative Working Group (CWG) supports the establishment of a consistent and clear nomenclature for use in IMRT. To this end, a glossary of words and phrases currently used in IMRT is given in the Appendix. Where clarification is needed, recommendations for new terminology are given.

As emphasized throughout this report, IMRT techniques are significantly more complex than many other traditional forms of RT, including conventional 3D-CRT. However, as discussed in later sections of this report, IMRT has the potential to achieve a much higher degree of target conformity and/or normal tissue sparing than most other treatment techniques, especially for target volumes and/or organs at risk with complex shapes and/or concave regions (Fig. 2).

It is important for the reader to fully appreciate that modern IMRT is more than just the use of non-uniform intensities in radiation fields. Beam modifiers such as wedges and compensators have been used for many years to

accommodate missing tissue and in some instances to shape dose distributions. However, as previously stated, modern IMRT is generally designed using inverse planning (or other methods) to optimize the shape of the dose distribution, with the capability of generating concave dose distributions and providing specific sparing of sensitive normal structures within complex treatment geometries. Thus, determining the optimum beam fluence is an integral component of IMRT. In fact, the central planning problem for IMRT is to determine the physically deliverable modulated beam fluence profiles that result in a dose distribution that most closely matches the desired one.

The clinical use of IMRT is in its beginning phase and has been implemented in only a few centers around the world. Much research and developmental work remains to be done to help make the application of this new technology straightforward and easy to perform. To date, only a few thousand patients have been treated using commercial (10–13) and university-developed (14–17) IMRT systems. The potential advantages of IMRT and inverse planning are relatively easy to demonstrate qualitatively in treatment planning exercises (see the section “Clinical Experience”), but careful comparative studies and clinical trials are needed to show that IMRT leads to improved outcomes. It is also possible that IMRT and inverse planning offer practical advantages that may not yet be fully appreciated by the radiation oncology community. That is, when IMRT is fully developed, the potential is significant for this integrated 3D planning and

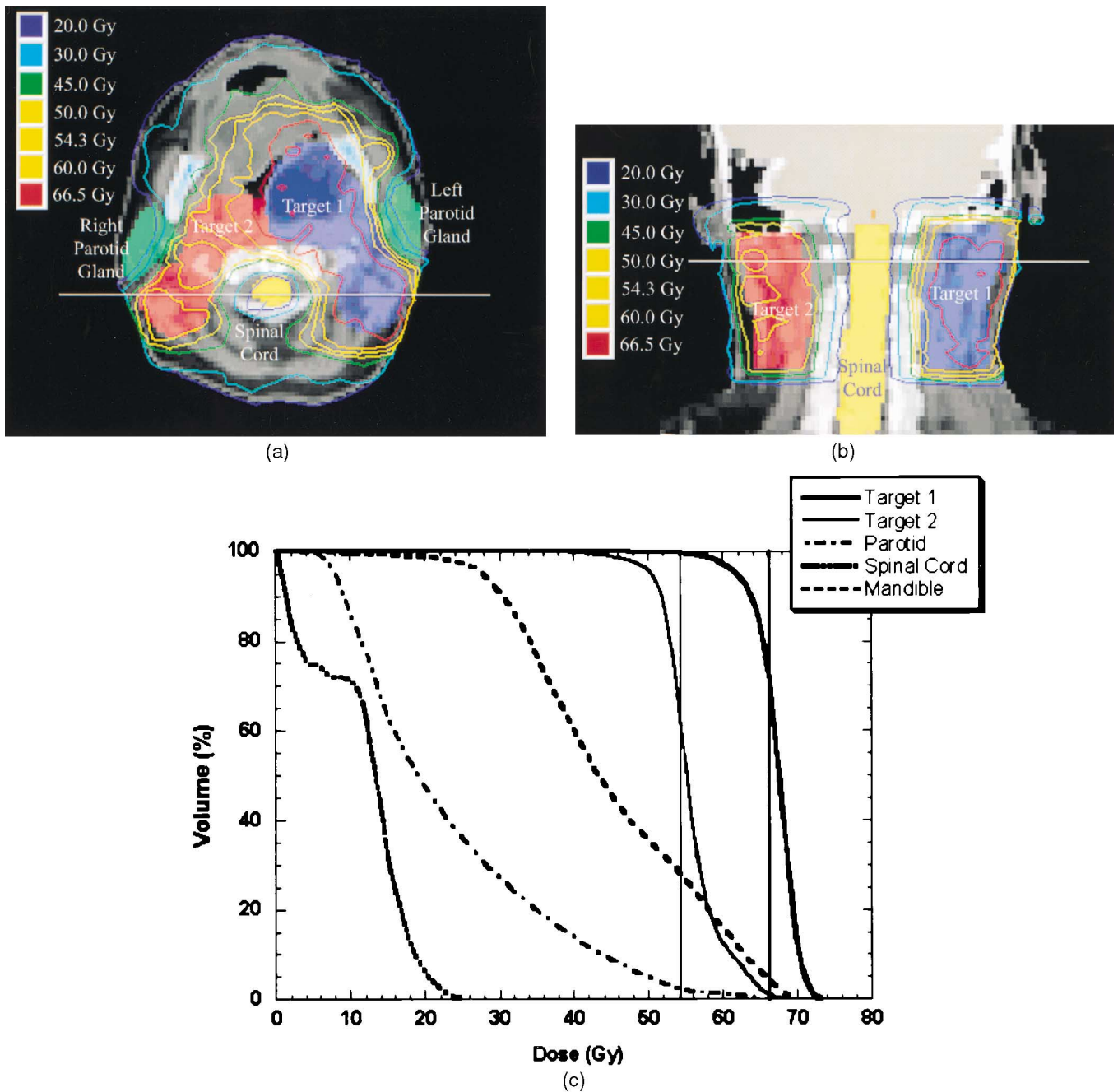


Fig. 2. Typical head-and-neck IMRT treatment plan showing conformal avoidance of the spinal cord and parotid glands while simultaneously delivering multiple dose prescriptions (66.5 Gy and 54.3 Gy) to the two target volumes. (A) Transverse cross-section. White line corresponds to the position of the coronal cross-section. (B) Coronal cross-section. White line corresponds to the position of the transverse cross-section. (C) DVHs of the target volumes and selected critical structures. Vertical bars indicate the prescription doses and highlight the increased dose heterogeneity often encountered as a consequence of conformal avoidance.

delivery technology to result in lower cost treatment machines and improved efficiencies in planning, delivery, and treatment verification, all of which will may make a valuable contribution to lowering the overall costs of RT while improving the therapeutic results.

This report is intended to create a snapshot in time of IMRT technology and its use. The intended audience is practicing physicians and medical physicists. We also

believe that many of the recommendations and suggestions may be of interest to IMRT equipment manufacturers and research funding agencies. We have tried to present a balanced summary that gives some historical perspective, addresses important IMRT issues, and highlights the most relevant publications. In some sections (e.g., "Facility Planning and Radiation Safety"), the reader will find that the depth of discussion and detail

presented is much more than in others. This was required to support specific recommendations but made for some unevenness in the writing.

## IMRT HISTORICAL REVIEW

The main technological precursors for the development of IMRT were the development of image-based 3D-RTP systems and the development of computer-controlled delivery systems.

### 3D treatment planning systems

Computerized RT planning was first reported >40 years ago (18). Early dedicated RTP systems depended on two-dimensional (2D) contour information and calculated doses based on relatively simple 2D dose models (19, 20). This type of planning was (and continues to be) widely used throughout the RT community. The first 3D approach to treatment planning dose calculation and display is credited to Sterling *et al.* (21, 22), who demonstrated a computer-generated film loop that gave the illusion of a 3D view of the anatomy and the calculated isodose distribution (2D color washes) throughout a treatment volume. van de Geijn (23, 24), Cunningham (25), Beaudoin (26), and Sontag and Cunningham (27) also performed early work in 3D dose-calculation models. Much of this work was eventually integrated into commercial RTP systems, but the full potential of image-based 3D treatment planning was not available to these early systems.

Reinstein *et al.* (28) and McShan *et al.* (29) took the first real step toward clinically usable 3D-RTP in 1978 with the development of the beam's-eye view display. The beam's-eye view display provides the planner with a view from the perspective of the source of the radiation beam, looking down the rays of the divergent beam, and results in a view of the anatomy similar to a simulator radiograph. At the same time, the introduction of CT scanning and its use for RT significantly improved the way patient anatomy could be specified in treatment planning (30, 31). In 1983, Goitein and Abrams (32) and Goitein *et al.* (33) demonstrated how CT data made possible high-quality color beam's-eye view displays and simulated radiographs computed from CT data (referred to as digitally reconstructed radiographs). Finally, between 1986 and 1989, several robust university-developed 3D-RTP systems began to be implemented in clinical use (34–37).

The additional development of 3D-RTP systems throughout the past 10 years, most importantly, including the commercial availability of 3D-RTP systems, has led to widespread adoption of 3D planning in many clinics. One of the keys to the acceptance of 3D-RTP throughout the community was a series of research contracts funded by the National Cancer Institute in the 1980s and early 1990s to evaluate the potential of 3D-RTP and to make recommendations to the National Cancer Institute for future research in this area (38). Each of these contracts funded a CWG to evaluate various aspects of 3D-RTP (Table 1). Important

Table 1. National Cancer Institute treatment planning collaborative working group research contracts

---

Evaluation of treatment planning for heavy particles (1982–1986)	University of Pennsylvania School of Medicine and Fox Chase Cancer Center
	Lawrence Berkeley Laboratory and University of California
	Massachusetts General Hospital
	M. D. Anderson Cancer Center, University of Texas
Evaluation of treatment planning for external beam photons (1984–1987)	University of Pennsylvania School of Medicine and Fox Chase Cancer Center
	Memorial Sloan-Kettering Cancer Center
	Massachusetts General Hospital
	Washington University, St. Louis
Evaluation of treatment planning for external beam electrons (1986–1989)	University of Michigan
	M. D. Anderson Cancer Center, University of Texas
	Washington University, St. Louis
Development of radiation therapy treatment planning software tools (1989–1994)	University of North Carolina
	University of Washington
	Washington University, St. Louis

---

developments and refinements in 3D planning technology came from these contracts, particularly plan evaluation software tools, such as dose-volume histograms (DVHs) (39, 40), and biologic effect models, such as tumor control probability (TCP) and normal tissue complication probability (NTCP) (41, 42) models, as well as efforts to stimulate and document the current state of knowledge about these effects (43, 44). Many of these features are crucial parts of plan optimization, which is critical to IMRT. Similar collaborative groups elsewhere in the world, for example, the Computer Aided Radiotherapy project in the Nordic countries (45), also contributed significantly to the development of 3D treatment planning.

### Precursors to IMRT delivery systems

Early IMRT delivery concepts were pioneered several decades ago. Particularly important were the early efforts of Dr. Shinji Takahashi and colleagues, from Nagoya, Japan (46). Their work illustrated some of the important concepts in both conventional 3D-CRT and IMRT delivery. Dynamic treatments were planned and delivered by Takahashi's group using what may have been the first multileaf collimator (MLC) system. The MLC system used a mechanical control system to conform the beam aperture to the projected target shape as the machine was rotated around the patient. Another pioneering effort in CRT was conducted by the group at the Massachusetts Institute of Technology Lahey Clinic (47–49), who independently developed an asynchronous portal-defining device similar to that of Takahashi (46).

The Royal Northern Hospital in England also pioneered an early CRT effort (50–52). The group developed a series

of cobalt-60 teletherapy machines in which the patient was automatically positioned during rotational therapy by moving the treatment couch and gantry during the radiation delivery using electromechanical systems. This was called the "Tracking Cobalt Project," because the planning and delivery system attempted to track around the path of disease spread and subsequently conform the dose distribution. Davy and Brace at the Royal Free Hospital in London extended the work in the 1970s and 1980s (53, 54).

The Joint Center from the Harvard Medical School also contributed to the development of computer-controlled CRT during the 1970s (55). Unfortunately, computer technology had not yet advanced to the degree required for practical implementation of traditional 3D-CRT.

Brahme (56, 57), Brahme and Ågren (58), and Cormack (59, 60) (working independently) presented many of the basic concepts related to the use of non-uniform intensity distributions to create improved dose distributions in a series of reports that discussed both planning/optimization issues and treatment delivery issues. In fact, many of these ideas were involved in the design of the Scanditronix MM50 Racetrack Microtron System, which was equipped with scanned beam control of beam intensity for both electrons and photons (61–63). However, with the exception of the continuing work by that group (e.g., the scanned MLC slit method studied by Kallman *et al.* [64] and Lind and Kallman [65]), most of the IMRT work that followed concentrated on the plan optimization side of the IMRT problem, for instance, the work by Bortfeld *et al.* (66). By the mid-1990s (and before much additional discussion had occurred in the literature about IMRT delivery methods), several other kinds of delivery techniques relevant to modern IMRT had evolved. These are summarized in the following section.

## IMRT DELIVERY TECHNIQUES

### *Scanned photon and electron beam IMRT*

The use of a computer-controlled scanned beam, available in the Scanditronix Racetrack Microtron System, was the first modern IMRT delivery technique described in the literature (56). In this system, limited resolution beam intensity modulation is performed using computer control of the beam-steering magnets that direct the high-energy electron beam onto the X-ray target. By controlling the angle and intensity at which the electron beam strikes the X-ray target, elemental bremsstrahlung X-ray beams are created and can be placed anywhere within the radiation field using a "scan pattern" that gives beam locations and intensities. Resolution of this technique is limited, because the full-width half maximum for even the 50-MV photon beam is several centimeters. Electron beams (especially the high-energy beams from 25 to 50 MeV) may also be used for IMRT with this technique, as demonstrated by Karlsson *et al.* (67) and Lief *et al.* (68, 69). Because only a few institutions have had access to this technology, much more work needs to be done to

fully investigate and evaluate the possibilities for scanned beam IMRT.

### *Tomotherapy IMRT*

The second IMRT delivery technique described in the literature defined an approach called *tomotherapy* (literally "slice therapy") by which IMRT is delivered using a narrow slit beam (70). This technique is very analogous to the tomography techniques used for CT and other such imaging systems. A temporally modulated binary mini-MLC of the type proposed by Mackie *et al.* (70) for tomotherapy IMRT was developed commercially (Peacock MIMiC, Nomos Corp.) (7, 71, 72). The Peacock system's MIMiC is mounted to a conventional low-energy megavoltage medical linear accelerator, and treatment is delivered to a narrow slice of the patient using arc rotation (Fig. 3). The beam is collimated to a narrow slit (approximately 2 cm × 20 cm), and beamlets of varying intensity are created by driving the MIMiC's leaves in and out of the radiation beam's path as the gantry rotates around the patient. A complete treatment is accomplished by serial delivery to adjoining axial slices. The clinical use of the Peacock system was first implemented at the Baylor College of Medicine in Houston, Texas (13). Since then, it has been implemented in a large number of clinics worldwide, and several other institutions have reported their experience with the Peacock IMRT system (10–12, 73). To date, this form of IMRT has been used to deliver more treatments than all other forms of IMRT combined. It has been referred to as *serial tomotherapy* (12) to distinguish it from the *helical tomotherapy* unit first proposed by Mackie *et al.* (70) and discussed in the next paragraph.

With serial tomotherapy, extreme accuracy in the motion of the couch is necessary, because the treatments are delivered in a series of contiguous arc strips. Positioning errors of as little as 1 mm can cause dose errors on the order of 10–20% in the abutment regions (74, 75). This issue is addressed by the helical tomotherapy treatment unit depicted in Fig. 4 (70). IMRT is delivered as the patient is moved through a ring-gantry in much the same way as a helical CT study is performed. Specifically, the beamlets are created using a temporally modulated binary mini-MLC similar to the MIMiC and a low-energy linear accelerator mounted in a modified CT scanner gantry. The original proposed design included a conventional diagnostic CT system mounted on the same gantry, allowing the simultaneous acquisition of a kilovoltage CT verification scan study. A prototype helical tomotherapy IMRT system (using megavoltage CT capability) is now under development at the University of Wisconsin and is scheduled for clinical implementation in the near future (76, 77).

### *Conventional MLC IMRT*

A conventional MLC under computer control can be used to deliver IMRT as follows. For a fixed gantry position, the

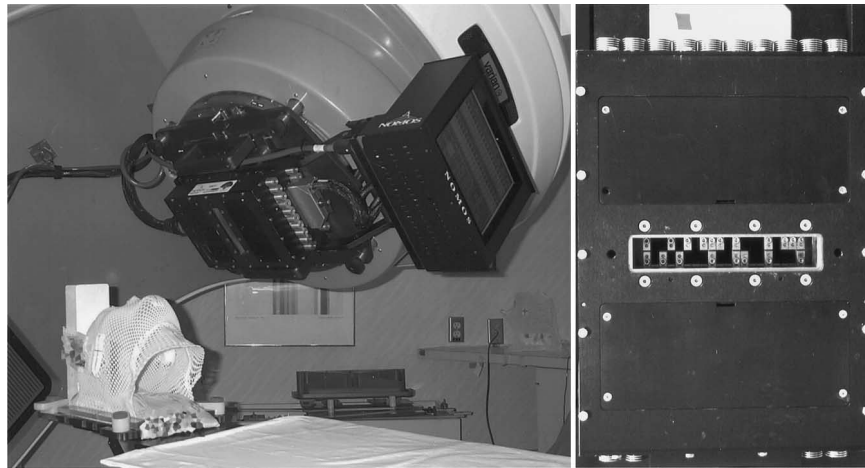


Fig. 3. Serial tomotherapy approach to IMRT. This form of IMRT uses a temporally modulated mini-MLC system such as the MIMiC (Nomos Corp.) shown here mounted to a conventional low-energy megavoltage medical linear accelerator. Treatment to a narrow slice of the patient is delivered by arc rotation. A complete treatment is accomplished by serial delivery to adjoining axial slices.

opening formed by each pair of opposing MLC leaves is swept across the target volume under computer control, with the radiation beam on, to produce the desired fluence profiles (Figs. 5 and 6a). The setting of the leaf pair opening and its speed for each MLC leaf pair are determined by a technique first introduced by Convery and Rosenbloom (78) and extended by Bortfeld *et al.* (79), Spirou and Chui (80), and Dirkx *et al.* (81). This IMRT approach, referred to as the *sliding window* or *dynamic MLC* (DMLC), was first implemented for clinical use at the Memorial Sloan-Ketter-

ing Cancer Center in New York (14). The IMRT CWG recommends that this form of conventional MLC IMRT be referred to as *DMLC*.

A second form of the conventional MLC IMRT approach uses a series of multiple segment fields, in which each field consists of a series of MLC shapes (*segments* or *subfields*) delivered from the same gantry angle, so that an intensity-modulated field intensity is delivered (Fig. 6b). The multiple segment fields are set up at selected orientations of the gantry under computer con-

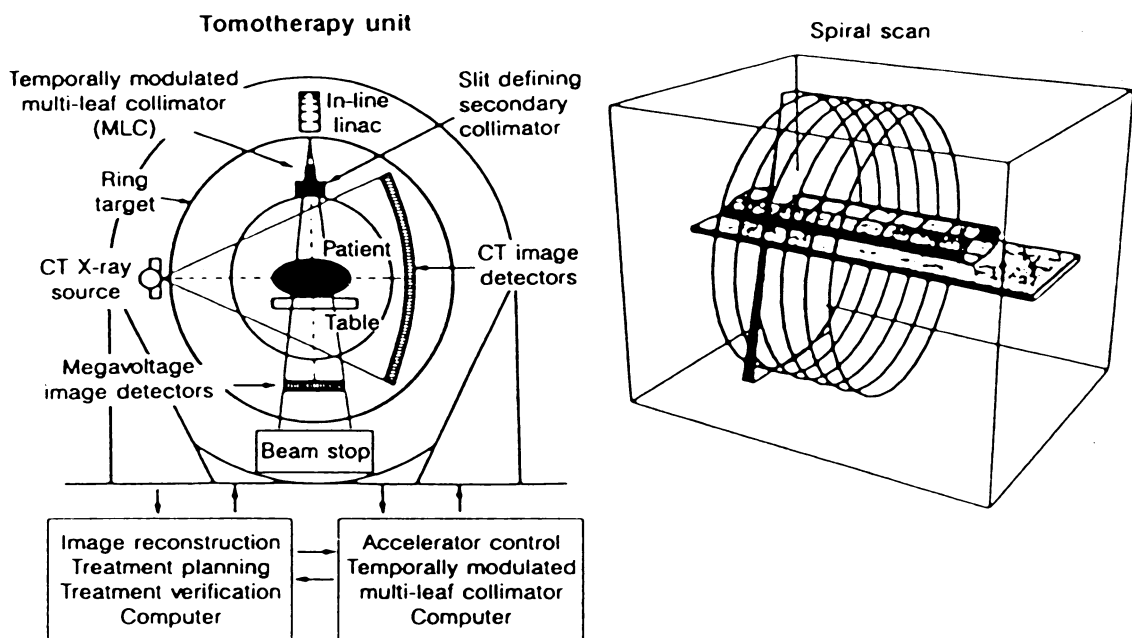


Fig. 4. Helical tomotherapy approach to IMRT. This new type treatment unit contains a low-energy megavoltage linear accelerator and a temporally modulated collimator system (similar to the Nomos MIMiC) mounted on a CT-like gantry. In addition, the system has the potential for enhanced verification using a CT X-ray source opposed by CT image detectors. The patient couch translates through the unit during treatment. (From Mackie *et al.* [70], with permission.)

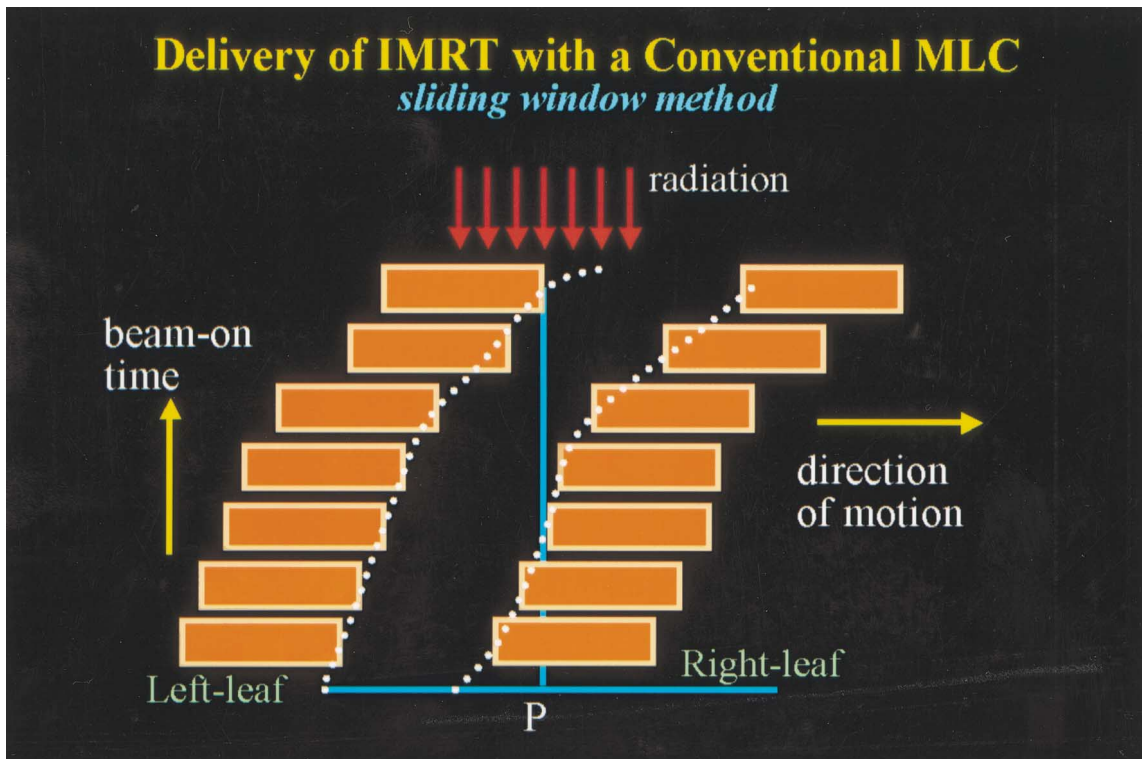


Fig. 5. DMLC technique of delivering IMRT (also referred to as the *sliding window* method). Dotted lines indicate positions of a leaf pair ( $x$  axis) as a function of beam-on time ( $y$  axis). As the beam is turned on (point a; see Fig. 6), both leaves move, with different speeds, from left to right. The point P begins to receive radiation when the right leaf edge moves pass over it (point b). It receives radiation until the left leaf blocks the beam (point c). By controlling the movement of the leaves and therefore the “beam-on-time” duration between b and c, one can deliver any desired intensity to point P, or any other point under this leaf pair.

trol. The radiation is turned on only when the MLC leaves are stopped at each prescribed segment position. This IMRT method has been referred to as *step-and-shoot* or *stop-and-shoot*. The IMRT CWG recommends this form of conventional MLC IMRT be referred to as *segmental MLC (SMLC)*. The leaf sequences can be determined by methods such as the one suggested by Bortfeld *et al.* (82) or Siochi (83). Another type of SMLC implementation makes use of multiple-shaped field segments to create the IMRT fields (15, 16). Most medical linear accelerator manufacturers are now offering SMLC-IMRT capability, and thus, widespread implementation of this form of IMRT is anticipated during the next several years.

A third conventional MLC IMRT approach, called *intensity-modulated arc therapy*, was described by Yu *et al.* (84–86). Instead of rotating a slit-field around the patient as done with tomotherapy, intensity-modulated arc therapy uses multiple irregular fields shaped with a conventional MLC during gantry rotation. Intensity-modulated arc therapy is planned as a sequence of static fields, every 5–10° apart, but delivered with multiple superimposing arcs. Within each arc, the MLC shape is continuously changed as a function of gantry angle on the basis of the results of optimization, such that the cumulative intensity distribution leads to the desired dose

distribution. This IMRT approach was first implemented for clinical use at the University of Maryland (87).

#### *Physical modulator (compensating filter) IMRT*

Several groups have reported on the use of a physical modulator to deliver IMRT (88–93). Filters can be designed using a 3D-RTP system to calculate the required thicknesses (along ray lines using an effective attenuation coefficient for the filter material and dose-ratio parameters for effective depths) to generate the desired IMRT fluence profile when the filter is placed in the radiation beam. Stein *et al.* (89) reported on the use of IMRT physical modulators fabricated using low-melting-point alloy poured into foam molds, which are cut using a computer-controlled cutter. In addition, Dubal *et al.* (94) recently reported on an IMRT physical modulator approach for the treatment of breast cancer. The physical modulator IMRT method has some advantages, including higher resolution in the direction normal to the leaf motion, higher precision compared with some MLC approaches, simpler quality assurance (QA), and no match-line problems. On the other hand, it has a relatively cumbersome and time-consuming manufacturing process and one must enter the treatment room to change the filter for each gantry orientation, thus increasing the time allocated for patient treatment. This approach will likely

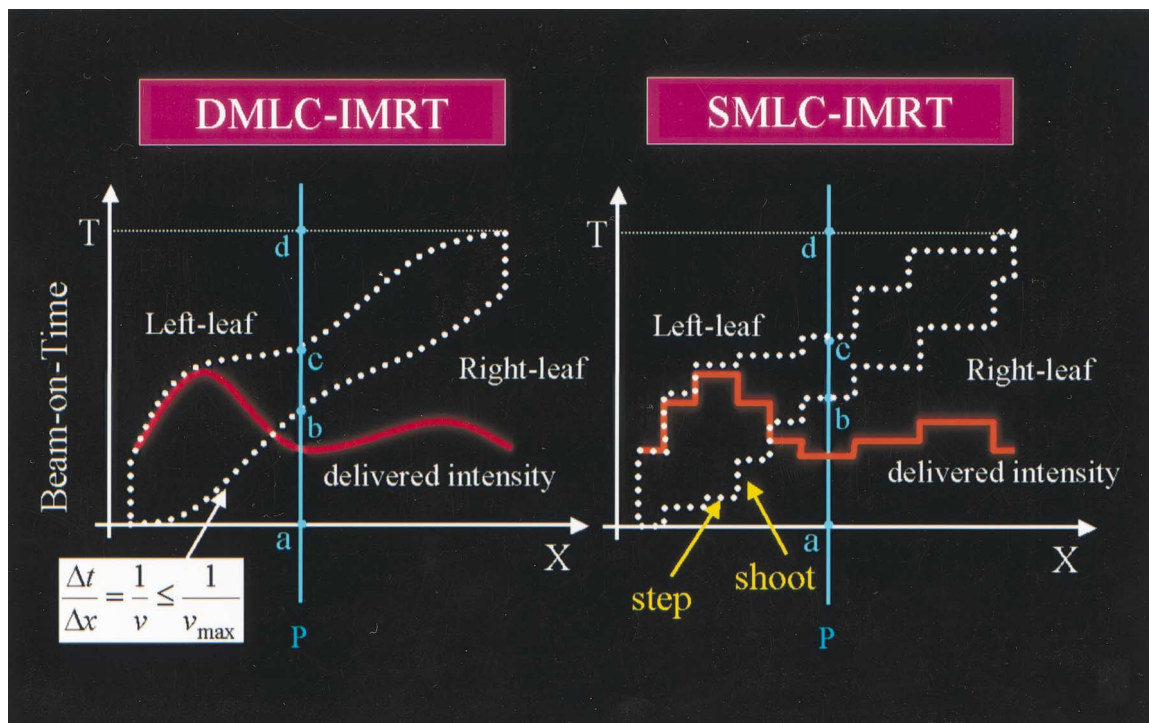


Fig. 6. (A) Intensity profile delivered by the leaves' paths of Fig. 5 (replotted here as dotted lines). In practice, a "leaf-sequencing" algorithm is used to translate the desired intensity profiles into a computer data file of the leaf positions as a function of MUs. (B) SMLC technique of delivering IMRT (also referred to as the *step-and-shoot* method). In the "step" phase, the leaves travel to discrete positions, then the radiation beam turns on in the "shoot" phase (i.e., alternate MLC movement and radiation delivery). The result is discrete intensity levels, the number of which depends on the "step" number.

serve only as an intermediate step in some institutions before other approaches to IMRT are adopted.

#### Robotic linear accelerator IMRT

The use of a small x-band linear accelerator, mounted on an industrial robot, a concept first developed for radiosurgery (95), has also been proposed as a treatment delivery device for sophisticated IMRT (96, 97). The robot would provide the capability for aiming beamlets with any orientation relative to the target volume, thus giving this IMRT approach more flexibility than any of those previously discussed. The treatment is specified by the trajectory of the robot and by the number of monitor units (MUs) delivered at each robotic orientation. This technology is not widely available at present, and significant research and development are needed to explore its use for IMRT.

### COMPUTER OPTIMIZATION

With the advent of computers, work on automated methods of plan optimization was initiated by numerous investigators, but did not result in widespread use. However, with the development of conventional 3D-CRT, interest in computer optimization was renewed, because the amount of image and graphic data the planner must deal with increased significantly, as did the computer hardware capabilities and software sophistication. In addition, as previously indicated,

IMRT requires a method of designing optimum non-uniform beam intensity profiles, a task for which computer optimization is indispensable. The use of computer optimization methods for IMRT plan design has been referred to *inverse planning* to distinguish it from the more iterative and interactive *forward planning* used in the planning of conventional 3D-CRT. During the past decade, major progress in computerized optimization for use in IMRT has been accomplished, led by Bortfeld *et al.* (66, 79, 98), Brahme (57, 99), Webb (100–103), Mohan *et al.* (104, 105), and others (71, 106). Other references of IMRT optimization are provided in the textbook by Webb (5).

In forward treatment planning, the beam geometry (beam orientation, shape, modifier, beam weights, etc.) is first defined, followed by calculation of the 3D dose distribution. After qualitative review of the dose distribution by the treatment planner and/or radiation oncologist, plan improvement is performed by modifying the initial geometry (e.g., changing the beam weights and/or modifiers, adding another beam), to improve the target dose coverage and/or decrease the dose in the organs at risk. This forward planning process is repeated until a satisfactory plan is generated. In inverse treatment planning, the focus is on the desired outcome (e.g., a specified dose distribution or even TCP and NTCPs) rather than how the outcome is going to be achieved. The user of the system specifies the goals; the computer (optimization system) then adjusts the beam pa-

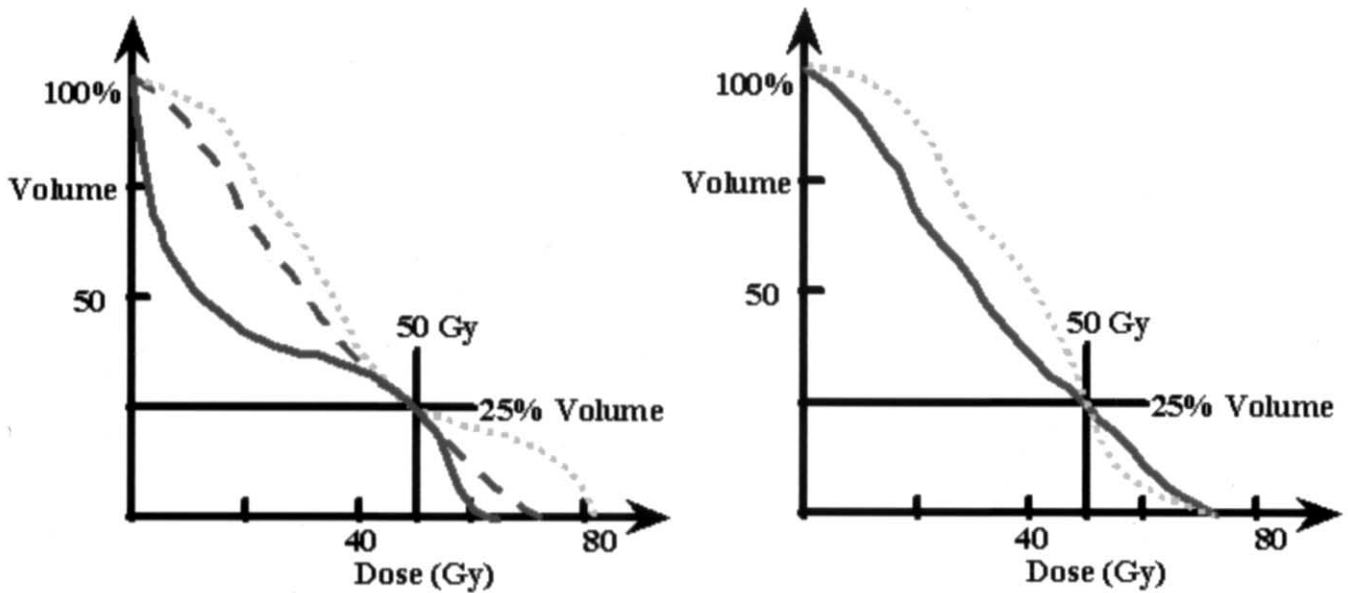


Fig. 7. Limitations of dose–volume-based optimization objective functions. (A) DVH for an organ at risk in which a criterion has been specified so that no more than 25% of the volume is to receive 50 Gy. All three DVHs shown meet this criterion; however, the DVH represented by the solid curve clearly causes the least damage. (B) This limitation can be overcome by specifying the entire DVH. However, different treatment techniques can result in dose distributions that could produce equivalent damage to a particular organ at risk, but have significantly different results for other organs at risk and/or the tumor (i.e., only one of these DVHs may be optimal so far as other organs and the tumor are concerned).

rameters (mainly the intensities) iteratively in an attempt to achieve the desired outcome. After review of the computer-optimized dose distribution, some modification of the desired outcome and adjustment of the relative importance of each end point might be needed if the physician is not satisfied with the dose to the target volume or organs at risk. Thus, one sees that both forward and inverse planning involve iteration to find the best plan.

To better understand the inverse planning method (computer optimization), it is helpful to separate the process into two components: (1) specification of optimization criteria (objective function and constraints) and (2) the optimization (search) algorithm used.

#### Objective functions

For inversely planned IMRT, the clinical objectives are specified mathematically in the form of an objective function (also called the score function or cost function). Computer optimization techniques are then used to determine the beam parameters (currently, often limited to the beamlet weights) that will most closely achieve the desired solution. The value of the objective function is the putative index of the goodness of the treatment plan. The term *score* or *cost* is often used to denote this value. Thus, the aim of optimization is to minimize (or maximize, depending on the choice of objective function) the score.

Some of the earlier attempts to optimize RT plans used objective functions based on dose distributions features (66, 98, 107–114). For example, one could choose to maximize the minimal dose to the target volume subject to a constraint

on the maximal dose to certain organs at risk. For simplicity, many investigators have used purely dose-based criteria for optimizing IMRT as well. However, it is recognized that, in general, the response of the tumor and normal tissues is a function of not only the radiation dose but also (to varying degrees depending on the tissue type) the volume subjected to each level of dose.

At present, most IMRT optimization systems use dose-based and/or dose–volume-based criteria. One method commonly used to create dose-based and dose–volume objective functions is based on minimizing the *variance* of the dose relative to the prescribed dose for the target volumes or dose limits for the organs at risk. Variance is defined as the sum of the squares of the differences between the calculated dose and the prescribed dose or dose limit. Thus, a typical dose-based or dose–volume-based objective function is the sum of the variance terms representing each anatomic structure multiplied with appropriate penalty factors (i.e., importance factors). This approach is sometimes referred to as a *quadratic objective function*.

If the physician knows the dose–volume relationships that are desired for the organs of interest, dose–volume-based objective functions may produce more appropriate plans than dose-based criteria. However, dose–volume criteria also have limitations (104, 115). Consider, for instance, an organ at risk for which the criterion has been specified so that no more than 25% of the volume is to receive 50 Gy (Fig. 7a). All three DVHs (Fig. 7) meet this criterion; however, the DVH represented by the solid curve clearly causes the least damage. One can argue that this

limitation can be overcome by specifying multiple dose–volume constraints or even the entire DVH. However, multiple DVHs (in fact an infinite number of them) could lead to an equivalent dose response for a particular organ (Fig. 7b). When this happens, DVHs usually cross each other as shown in Fig. 7. Optimization based on each of these biologically equivalent DVHs would, in general, lead to different dose responses in other organs and the tumor. Only one of the DVHs may be optimum so far as the other organs and tumor are concerned. Thus, constraining the search to a single DVH for an anatomic structure may miss the overall optimal solution.

Another weakness of quadratic (i.e., variance) dose- and dose–volume-based objective functions, as typically used, is that neither adequately represents the nonlinear response of tumors or normal structures to dose, especially for arbitrary inhomogeneous dose distributions. For instance, if a single voxel or a small number of voxels in a tumor receive a very low dose, it would not have a significant effect on the IMRT plan score. However, the tumor control probability would be greatly diminished as a result of the cold spot. Stated in a different way, for dose- or dose–volume-based objective functions, the penalty imposed for the failure to achieve the prescribed dose is proportional to the dose difference (or the square of the difference), rather than to the loss of tumor control, which would be more appropriate. Such limitations have led a number of investigators to consider models for predicting biologic and dose–response indexes that could be used to supplement dose and dose–volume criteria (104, 105, 116–122). One way to cast the objective function in terms of the clinical and biologic criteria is to use indexes such as TCP, NTCPs, and the equivalent uniform dose (122). Objective functions based on biologic and dose–response indexes for IMRT optimization do not represent the state-of-the-art of IMRT clinical practice. They are a topic of on-going investigations and are not discussed further in this report.

In addition to dose, dose–volume, and dose–response information, it may be necessary to include other important factors in the objective function, such as plan complexity and other nondosimetric factors that affect how the patient should be treated. In a method proposed by Kessler *et al.* (123) and Fraass *et al.* (15), the objective function is created from the combination of many different components, called *costlets*. This very general method can combine dose, DVH point, TCP, and NTCP-related costlets into an overall score function. This type of construct may have the flexibility needed for a clinically relevant score function, but it also shares all the disadvantages of each of the individual costlets used.

In summary, in the current state-of-the-art, dose–volume-based objective functions have become an accepted standard. In general, they produce satisfactory plans, and their continued use is recommended until dose–response-based objective functions are shown to have a clear and significant advantage. Many issues regarding IMRT computer optimization need additional investigation. Objective functions

that are more clinically relevant need to be defined and their parameters determined for each combination of treatment site, IMRT delivery technique, and other clinical factors (i.e., establishment of IMRT class solutions). The determination of parameters of an objective function (whether dose–volume-based or dose–response-based) that may be applied to all patients presenting with a specific class of clinical indications is an important, but at the same time a daunting task, especially when the number of such parameters is large (multiple organs and multiple dose–volume constraints per organ). Research is needed to systematize the determination of these parameters. Furthermore, the limitations of the dose-, dose–volume-, and dose–response-based objective functions need to be determined. Most importantly, accurate dose–volume–response data for each organ and tumor type need to be accumulated prospectively and analyzed to develop more dependable dose–response-based optimization criteria.

#### *Computer optimization (search) process*

The process of the optimization of intensity distributions may be carried out using one of several mathematical formalisms and algorithms (referred to as *optimization* or *search methods*). The choice may depend on the nature of the objective function used, on the scope and number of parameters to be optimized, the accessibility of each particular method, and individual preference. In the pioneering work on IMRT optimization, Brahme *et al.* (99, 124) used “radiation kernels” to first produce optimum dose distributions and then, using the inverse back projection technique borrowed from image reconstruction methods, to obtain intensity distributions that would lead to the best approximation of the optimum dose distribution. Since then, a large variety of methods have been evaluated. They fall into two basic categories: gradient methods and stochastic methods.

The following is qualitative explanation of how a typical optimization algorithm works. (This explanation is specifically for gradient methods, but, with some exceptions discussed later, applies to stochastic methods as well.) Each beamlet is traced from the source of radiation through the patient. In general, only the beamlets that pass through the target volume need to be traced, plus a small margin around the target volume that is assigned to ensure that the lateral loss of scattered radiation does not compromise the treatment. All other beamlets are set to a weight of 0. The patient’s 3D description is divided into small volume elements or voxels. The dose in each voxel is calculated for an initial set of beamlet weights. The resulting dose distribution is used to compute the value of the objective function (i.e., the score). If the change in beamlet weight results in an improved score, the proposed change in weight of that beamlet is accepted, and if not, the change is rejected (depending on the search method, see below). Because the improvement in the plan at each point comes from beamlets from many different directions and each beamlet affects many points, only relatively small changes in beamlet weight are permitted at one time. This process is repeated

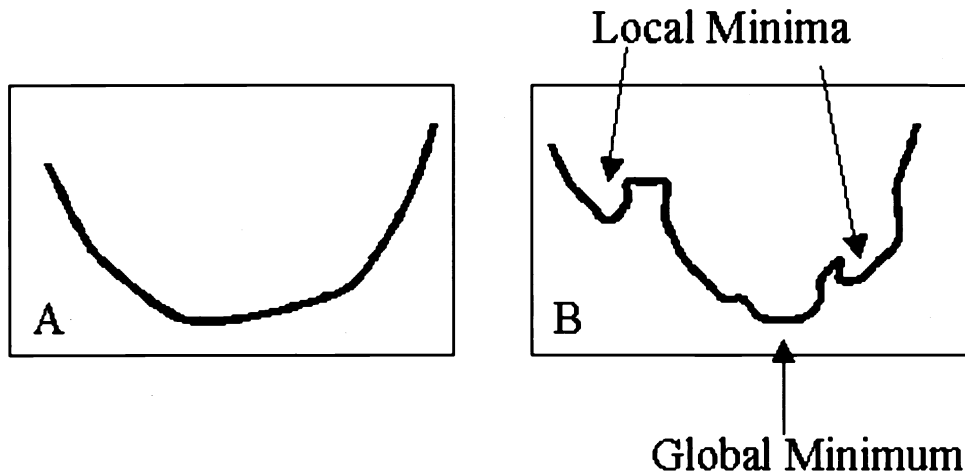


Fig. 8. Objective functions with (A) a single minimum and (B) multiple minima.

for all the beamlets. At the end of each complete cycle (an iteration), a small improvement in the treatment plan presumably results. The new pattern of beamlet intensities is then used to calculate a new dose distribution and a new score of the objective function, which is then used as the basis for additional improvement in the next cycle. This iterative process continues until no further improvement takes place; at that time, the optimum plan is assumed to have been achieved.

*Gradient techniques* are by far the fastest computationally (106, 125–128). However, the use of a gradient technique assumes that there is a single extremum (a minimum or a maximum, depending on the form of the objective function) (Fig. 8). This is the case for a quadratic objective function (based on variance of dose) when only beamlet weights are optimized. For other cases, it may be necessary to determine whether multiple extrema exist, and whether these multiple extrema have an impact on the quality of the solutions found. Multiple extrema have been found to exist when beam directions are optimized and when dose–response-based objective functions are used to optimize the weights of uniform beams (104, 129, 130). One can expect that multiple minima also exist when dose–response-based objective functions are used to optimize IMRT plans. Using simple schematic examples, it has also been shown that multiple minima exist when dose–volume-based objectives are used (131). When multiple extrema exist, the gradient search methods will converge to the nearest extremum. The treatment plan corresponding to this extremum may be far from the best solution possible and may be totally unsatisfactory. However, although this may be the case in theory, the existence of multiple minima has not yet been found to be a serious impediment in dose–volume- or dose–response-based optimization of IMRT plans using gradient techniques. If multiple minima are found to be a factor, some form of stochastic optimization technique (see next paragraph) may need to be considered.

The most commonly used stochastic technique is *simulated annealing* or its variation *fast simulated annealing*

(102–104, 111, 129). Other forms of stochastic approaches such as “genetic algorithms” have also been proposed (132). In principle, the simulated annealing technique and other stochastic approaches allow the optimization process to escape from the local extrema traps and thus find the global extrema, as shown in Fig. 8; however, this is true only if a large number of configurations are tested. Practically, there is no guarantee that the absolute optimum will be found, only that the best solution among those examined will be found. Furthermore, stochastic techniques tend to be relatively slow. Nevertheless, some commercial systems have implemented the simulated annealing approach for IMRT optimization (72).

In summary, gradient search algorithms are fast and have so far been able to produce satisfactory results. Although multiple extrema are known to exist, their existence has not, in general, been shown to be an impediment in achieving satisfactory solutions. Continuing research is needed to determine whether the use of slow stochastic methods will lead to a significant improvement in the results. In the meantime, it is recommended that, for efficiency reasons, gradient methods be used in routine clinical practice of IMRT.

#### *Leaf sequence generation*

Most current IMRT planning systems produce a description of the beam intensity patterns. These intensity distributions are then used in a process called *leaf sequencing*, in which an algorithm attempts to define the shapes (for SMLC–IMRT) or trajectories (for DMLC–IMRT) of the MLC leaves required to create a deliverable intensity distribution that gives an intensity distribution as close as possible to the distributions obtained from the optimization system. Methods for SMLC–IMRT leaf sequencing have been described by Galvin *et al.* (133), Bortfeld *et al.* (82), Boyer and Yu (134), and others. Use of dynamic leaf motion has been described by Spirou and Chui (80), Dirkx *et al.* (81), and others. Leaf sequencing for tomotherapy is particularly simple, because the leaves are rapidly driven open or closed

with the intensity through the leaf position proportional to the time it is open.

To deliver a predictable dose distribution, a number of other refinements are needed in an accurate MLC leaf-setting sequence to account for effects such as field flatness, the relative output factor of the MLC leaves, penumbra, phantom scatter effects, leaf leakage, rounded leaf ends, and back scatter into the transmission ion chamber (80). Prominent among these is the consideration of leaf leakage. The leakage dose delivered along the profile can be calculated once a first approximation of the sequence has been computed. This leakage is a low-dose profile. The leakage-dose profile can be subtracted from the desired profile and the leaf-setting sequence recomputed using the corrected profile. Other modifications of the leaf-setting sequence can correct for the tongue-and-groove effect (135, 136). Integration of more detailed delivery-related effects and limitations into the overall optimization process is an area requiring continued research and development.

## DOSE DISTRIBUTION AND MU CALCULATIONS FOR IMRT

The calculation of the dose distribution associated with IMRT delivery is a critical aspect of the IMRT optimization and delivery processes. The calculated dose distribution from each candidate set of plan parameters is evaluated at each iteration of the optimization process, and the objective function values (costs or scores) for the iterative optimization are typically obtained by analysis of the dose distribution. After the optimized plan is obtained, another dose calculation/optimization procedure, called leaf sequencing, is performed to account for the dose calculation or physical limitations in the delivery script. Typically, the actual MUs used to deliver each of the IMRT fields are calculated as part of this process, because the leaf-sequence corrections may depend on the number of MUs. Often, the results of the leaf-sequencing algorithm are input again into a dose-calculation algorithm to generate a dose distribution that should represent the actual dose distribution delivered to the patient. In each of these steps, the speed, accuracy, and generality of the dose-calculation algorithms used for each step must be considered, because limitations may affect the true accuracy of the results.

During the iterative optimization part of the process, severe demands are placed on the dose-calculation algorithm. First, the number of iterations through the dose calculation (for different beamlet intensity distributions) may range from hundreds (for gradient search methods) to tens or hundreds of thousands (for the stochastic methods such as simulated annealing). Therefore, the speed of the dose-calculation method can often be crucial, and severe approximations or limitations are often imbedded in the calculation algorithm used within the optimization loop. A second limitation is that most current dose-calculation algorithms used within the optimization usually consider the intensity or fluence distribution to be an ideal set of beamlet

intensities, and rarely (if ever) are any of the realistic limitations associated with the delivery of those intensity distributions included in the calculation results. A third limitation involves the number of dose points inside the volume of interest that are actually calculated, because increasing the number of points significantly reduces the speed of the dose calculation for each iteration; this leads to the potential for resolution problems that often cause inaccurate evaluation results (in the objective function) rather than just limiting the spatial resolution of the dose distribution, as was the case when the isodose lines were the main evaluation criteria for a plan. Finally, given the ability of the optimization algorithm and IMRT delivery to react to small influences within the field (i.e., the accuracy of the dose-calculation algorithm with respect to issues such as heterogeneities within the patient, density corrections, surface dose/buildup region accuracy, patient setup uncertainty, and organ motion), as well as the potential for use of small "beamlets" that are much smaller than normally used radiation fields, the inaccuracy of the dose-calculation algorithm in any of the above situations may lead to significant reductions in the quality of the calculated-dose distribution and the plan that results from the optimization. Therefore, significant attention must be given to the various dose-calculation compromises and decisions that are incorporated in any optimization or inverse planning system.

### *Calculation algorithm types*

From the perspective of IMRT, four types of dose-calculation algorithms may be described. Many calculation algorithms can be classified broadly as broad beam algorithms, because they are intended for use with flat or wedged fields and do not really apply to the variable intensity situation used for IMRT. These algorithms are usually not appropriate for the significantly more complex intensity distributions often used in IMRT and should be used only with great care. For each IMRT beam, the intensity pattern for the beam can be modeled as a 2D map of energy fluence incident on a patient. The map can be divided into discrete beam elements called beamlets (sometimes called *bixels* or *rays*). A beamlet could correspond to a finite region of a compensator, a portion of the travel of a leaf of a conventional MLC, or a leaf of a temporally modulated binary mini-MLC. The dose distribution resulting from the intensity or fluence through each beamlet must then be calculated.

One of the most commonly used IMRT dose-calculation algorithm types can be described as a simple pencil beam method and is generally part of a broader class of correction-based dose-calculation algorithms (137, 138). Correction-based models depend on empirically measured data for a limited number of situations and then correct the dose distribution for the presence of the beam modifiers, contour corrections, tissue heterogeneities, and other issues encountered in treatment planning of real patients. A good example of this type of model is the finite-size pencil beam algorithm described by Bourland and Chaney (139) and extended by Ostapiak *et al.* (140). The dose resulting from each individ-

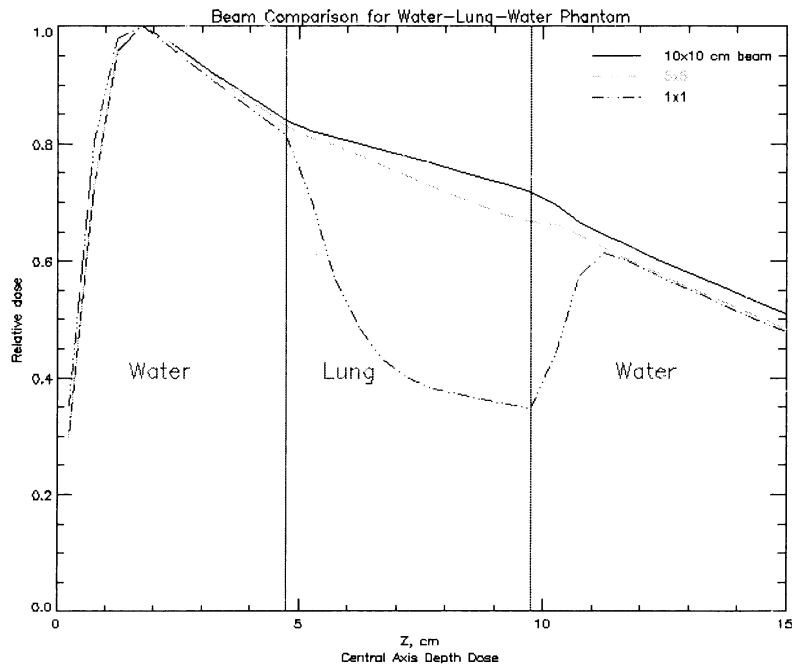


Fig. 9. Set of central axis 4 MV X-ray depth-dose curves computed for a variety of field sizes in a water phantom with a lung-equivalent slab ( $0.3 \text{ g/cm}^3$ ). The  $1 \text{ cm} \times 1 \text{ cm}$  field size is typical of the pencil beam size used in IMRT.

ual beamlet is calculated using the product of the inverse square law, the Tissue-Maximum Ratio (TMR) for the pencil beam, an off-axis ratio, the appropriate output factor, the MUs delivered, and various constants or other correction factors. Models with this kind of simplicity offer significant speed advantages for use in the optimization code but have varying limitations in accuracy.

A third kind of calculation algorithm is based on the kernel-based models, which directly compute the dose in a phantom or patient. Typical of this type of model are convolution/superposition algorithms that can take into account beam energy, geometry, beam modifiers, patient contour, and electron density distribution (141–145), although there are also pencil beam approaches (146) that bridge the gap between the empirically based correction models (like the finite-size pencil beam) and true kernel-based convolution models. Unlike correction-based methods, kernel-based approaches do not first compute the dose in a water phantom and correct the water dose for the treatment circumstances. Both the convolution method and the Monte Carlo method (discussed below) compute the dose per unit energy fluence (or fluence) incident on the patient.

Convolution methods are capable of accounting for electronic disequilibrium effects (141–145) and may more accurately deal with inhomogeneities and other complex aspects of IMRT dose calculations than the models described above. Fig. 9 illustrates the potential for large differences in the dose due to inhomogeneities for small beamlets. In this example (water phantom with a lung-equivalent slab), the depth-dose for the  $10 \text{ cm} \times 10 \text{ cm}$  field is only slightly perturbed because of the reduced attenuation of the primary photons. However, the depth-dose for the  $5 \text{ cm} \times 5 \text{ cm}$  field

has a reduced dose because of the streaming of electrons laterally, and the  $1 \text{ cm} \times 1 \text{ cm}$  field, typical of the area of an IMRT beamlet, shows severe perturbation because of electronic disequilibrium. The perturbing effect of electronic disequilibrium increases with the beam energy (147, 148). It is evident from this simple example that the development of IMRT plans requires a dose-calculation method that can accurately predict electronic disequilibrium effects. Although it is clear that the improved dose-calculation accuracy afforded by the convolution-type calculations may be important for IMRT, the long calculation times make this difficult. Currently, many optimization approaches do not use these more accurate calculations, or only use them at the end of the optimization to calculate the final delivered dose distribution. Only one group has reported the use of full convolution/superposition calculations within the optimization iteration loop (149).

Recently, significant progress has been made in the development of Monte Carlo calculation algorithms for photon beams that are fast enough to compete with other current methods (150–153). In several situations, the Monte Carlo method is likely to be even more accurate than the convolution method (154). For example, multiple scatter (second and higher order scatter) may be perturbed near the surface of a patient and the Monte Carlo method may be able to account for this as long as the number of simulated particles (called histories) is sufficient to compute the multiple scattered photon dose accurately. In addition, the “density scaling” method (154) used by the superposition/convolution methods to correct for heterogeneities may not be adequate for primary electrons set in motion, especially in higher atomic number materials, such as bone or metal prostheses,

in which the electrons may be scattered laterally considerably more than in water. Direct Monte Carlo simulation may be the only option for achieving accurate dose computations in these complex situations. However, the application of Monte Carlo methods to optimization for IMRT is an area that requires much more work before relevant results will be available.

#### *Important issues for IMRT dose calculations*

The following features should be explicitly modeled in all IMRT dose-calculation algorithms to achieve reasonable accuracy, although, at present, many IMRT dose-calculation algorithms compromise many of these issues:

Finite source size

Extrafocal radiation generated mainly in the primary collimator and the field-flattening filter (155)

Beam spectrum and the change in spectrum with lateral position

Beam intensity variation across the field (e.g., the beam horns)

Transmission through independent or dependent collimator jaws and MLC (156)

MLCs vs. Cerrobend blocks (with blocking tray)

Wedges and compensators (including the spectral hardening they produce)

Dynamic wedge

Scatter outside the field (related to extrafocal radiation [155])

Electron contamination

Delivery specific limitations and issues

All the above issues may influence the accuracy of the proposed optimized IMRT plans. The clinical importance of each of these factors within the optimization context should be the subject of further research.

Within the context of optimization, dose calculation speed is a critical issue. Currently, any algorithm will make speed vs. accuracy compromises to allow the optimization algorithm to work within a reasonable time. However, for any dose-calculation algorithm, any approximation that compromises dose-calculation accuracy for the sake of speed must be validated or characterized, so that the implications of the compromises on the clinical results will be understood. During the coming years, improvements in calculation speed and accuracy are expected. For example, the time required to perform the Monte Carlo simulation depends only on the number of histories through a region and not on the number of beams computed. Thus, for IMRT, which is calculated using many independent beam directions, Monte Carlo calculation times may not be too unreasonable, because the number of histories per beam can be reduced in proportion to the number of beams simulated (157). For the coming years, the investigation of the tradeoffs and implications of dose-calculation approximations will be an important research area.

#### *MU calculations for IMRT*

Conventional MU calculation methods were designed for computing the dose from measured dose information. These methods perform very well when the beam is rectangular and incident perpendicular to the water phantom. They perform less well when there are beam modifiers like compensators, contour corrections, and heterogeneities. In IMRT, the beam shapes are unlike anything used conventionally (158). Rather than lacking electronic equilibrium only near the surface and the boundaries of fields, most of the field is in a state of disequilibrium. Thus, methods such as the Clarkson summation technique and off-axis factor may not be accurate for IMRT fields.

One of the most difficult problems with correction-based techniques is the separation of scatter from the phantom from scatter from the head of the machine. This is not a problem for the convolution and Monte Carlo methods, which implicitly compute the contribution of phantom scatter, leaving only the contribution of head scatter to determine. In many implementations, the kernel-based algorithms determine the energy fluence per MU that is emitted by the machine and is thereby incident on the patient (137, 159). There are beginning to be accurate ways to model the emitted energy fluence; however, it is also possible to infer it from dose measurements without requiring the measurement of the dose with a buildup cap or a miniphantom (160–163). None of these methods is currently accepted as the standard, and most institutions that treat patients with IMRT routinely confirm the actual MU used for clinical treatments for each patient. It is clear, certainly, that more work in the area of MU calculations for IMRT is needed.

#### *Recommendations: IMRT dose calculations*

The following list summarizes the IMRT CWG recommendations regarding dose-calculation algorithms for IMRT:

1. Kernel-based models and Monte Carlo simulation should be further developed for use in dose computation for IMRT. Both methods intrinsically model the energy fluence incident on a patient during IMRT and take into account the transport of secondary particles. Both methods account for electronic disequilibrium, which occurs even at the central axis in finite-size pencil beams. Additional research to make accurate convolution/superposition and Monte Carlo algorithms suitable for routine clinical use should be encouraged.
2. The model of the incident beam should take into account many effects, including the finite size of the source, extrafocal radiation, disequilibrium effects in inhomogeneities, changes in the surface dose distribution, transmission through collimation systems, and many other effects.
3. Traditional MU calculations based on broad-beam data, such as tissue-phantom ratios, may be inappropriate for IMRT. Instead, accurately measured pencil beams or kernel-based methods that compute the dose per incident

energy fluence and are calibrated by measurements to obtain the energy fluence per MU produced by the beam in reference conditions appear to be better suited for IMRT. However, much work in this area is still required.

### IMRT ACCEPTANCE TESTING, COMMISSIONING, AND QA

In many ways, the issues that must be addressed during acceptance testing and commissioning of IMRT planning and delivery systems are analogous to those necessary for conventional 3D-CRT. 3D-RTP systems, for example, have in common the requirement for consistently keeping track of patient-specific information, such as name and identification number, patient image data sets, contours, and dose displays. Both IMRT and conventional 3D-RTP systems calculate 3D dose distributions, and the accuracy (magnitude and position) of those dose distributions must be verified before their clinical use. The American Association of Physicists in Medicine (AAPM) has recently published a task group report (TG 53) describing the acceptance testing and commissioning of 3D-RTP systems, and the reader is referred to that report for a discussion of features in common with IMRT planning systems (164). The acceptance testing, commissioning, and periodic QA effort outlined by the AAPM TG 53 report is quite extensive, and all of that effort, in principle, applies to IMRT planning systems. Thus, the amount of work by the medical physicist to clinically implement an IMRT system must not be underestimated. Adequate time and resources must be made available.

At least two aspects of IMRT distinguish it from conventional 3D-CRT: (1) the optimization process in the planning phase, and (2) the use of non-uniform and customized fluence distributions in the treatment delivery. Computer optimization algorithms are an entirely new kind of tool to be added to the treatment planning process and will require the development of new techniques for commissioning, because, in principle, many inverse planning search algorithms are based on stochastic methods that may not achieve exactly the same answer each time, even for the same initial conditions. Because the development of these optimization systems is quite new, the commissioning and testing techniques for these systems have not yet been fully developed, and only a cursory discussion of them is possible in this report. For example, the question of whether the optimization system always finds the truly best plan cannot be answered at this time for realistic objective functions that have multiple minima. This is clearly an issue for which more research is necessary. However, at worst, nonoptimal plans will be created, which should be readily recognizable. The remainder of this section discusses QA for the non-uniform fluence distributions used in IMRT.

#### *Acceptance testing of the IMRT treatment planning system*

As with many validation procedures, the acceptance test criteria are typically expressed by pass-fail criteria, in which

the system output is compared against criteria that have been developed and accepted by the medical physics community. For traditional treatment planning systems, comparisons are typically made between calculated and measured dose distributions using the Van Dyk *et al.* (165) published criteria for dose-distribution comparisons that take into account variations in dose-distribution gradients. For low-dose gradient regions, the comparison is based on the difference between the measured and calculated doses, with a criterion of 2% for photon beams along the central axis and 3% for relative comparisons. In high-dose gradient regions, the measured dose precision is affected by the uncertainty in the spatial precision of the measurement. The AAPM TG 53 report (164) generalized and expanded on the concepts in the Van Dyk work and suggested a method for characterizing the accuracy desired for more complex planning situations. However, IMRT is even more complex, because very high-dose gradients may be created by individual intensity-modulated beams. One method that may help evaluate this kind of situation is the distance to agreement (165). For each measurement point, the calculated dose distribution is examined to determine the distance between a measurement point and the nearest point in the calculated distribution exhibiting the same dose. Note that care must be used in applying this concept to individual beam dose distributions, which are then added up, because the final dose distribution in the end is the result that must be confirmed.

Dose-distribution comparisons are typically performed using manual techniques, such as by examining the dose distribution on the computer screen or by printing one-dimensional or 2D hard copies of both the calculated and the measured distributions. Although these techniques yield sparse quantitative data, they are often the only comparisons available to the physicist. Treatment planning tools for comparisons and evaluation of dose calculations, measurements, and other QA activities have been described by Fraass *et al.* (166), Harms *et al.* (167), and Low *et al.* (168); however, most treatment planning companies have not yet implemented dose-distribution measurement comparison software to enable a more thorough evaluation of the calculated dose distributions. The CWG recommends that these kinds of quantitative tools be implemented by manufacturers to help the physicist perform more quantitative plan comparisons for IMRT and 3D-CRT.

In addition to the direct quantitative evaluation of the IMRT planning system, the commissioning process should include a determination of the effects of the input parameters on the optimized dose distribution (169). This evaluation should be conducted using clinical patient scans and target and organ-at-risk volumes and should be completed for each treatment site to be used for IMRT. Although a comprehensive evaluation of the input parameters may not be possible, an attempt should be made to reduce the available parameter space to assist treatment planners in developing the initial treatment plan parameters.

As indicated earlier, no accepted criteria are available as

yet for acceptance testing of the quality of the dose distributions produced by automated optimization. The development of acceptance criteria for IMRT planning systems will be critical for its widespread clinical implementation. Without such criteria, quantitative comparisons between different IMRT planning systems will be difficult. The CWG believes it would be useful to establish a standard set of phantoms with defined geometries (target volumes and organs at risk) and specified optimization protocols and evaluation criteria to enable meaningful comparisons between different IMRT planning systems and to develop criteria for acceptance testing and commissioning.

#### *Verification of IMRT dose distributions*

At the heart of acceptance testing and commissioning procedures are dose measurements and their comparison with IMRT planning system calculations. Dose measurements to be used for testing IMRT systems must be conducted using non-uniform beam fluences, and the consequences of those non-uniform fluences on dose measurements must be considered by the medical physicist. The appropriate selection of detectors and the accurate determination of the detector spatial location are critical to achieving accurate results when IMRT systems are tested and commissioned.

The spatial location of measurement points must be known to high accuracy to enable quantitative evaluation of the calculated doses at those points. The spatial relationship between the dosimeter and the phantom are required, as is the relationship between the accelerator alignment mechanism and the phantom. Provided the phantoms are accurately fabricated, the machine drawings of any special phantom used are the best means for determining these relationships, although physical measurements or CT scanning can also be used. For example, if an anthropomorphic phantom is used for RTP system commissioning and machine drawings are not available to provide the dosimeter positions, physical measurements are required to determine the 3D location of the dosimeters relative to the alignment system.

The position of the calculated doses must also be known. The IMRT planning system should be capable of providing the coordinates of the calculated doses, and these can be used to identify the most appropriate calculated doses to compare against measurement. Because IMRT provides very nonintuitive fluence distributions, and no mechanism currently exists for independently verifying that the delivered fluence yields the desired dose distribution, an independent determination of the measured and calculated dose distribution coordinates is essential.

For conventional 3D-CRT, a significant portion of the dose-calculation algorithm verification testing can be conducted using static beams. Because the depth-dose and divergence behaviors are well characterized, a relatively sparse measurement data set is sufficient to accurately characterize the beam dose distribution. For example, a point dosimeter, such as an ionization chamber, is typically

scanned in a water phantom, acquiring a series of linear profiles, which are interpolated to obtain a planar dose distribution. A single-point dosimeter is capable of acquiring dose measurements of sufficient density to characterize the beam because the beam fluence is constant with respect to time.

IMRT dose distributions are characterized by complex 3D dose gradients and a time-dependent fluence delivery, placing severe limitations on the dosimeters and techniques used to characterize IMRT dose distributions. Careful analysis of the available dosimeters is required before developing a QA program for IMRT. Although there are promising 3D water-equivalent dosimeters, most are limited either by their spatial resolution, sensitivity, and noise or by nonwater equivalence. Currently, no single dosimeter is capable of providing all the necessary dose measurements; thus, compromises must be made.

Today, the benchmark dosimeter for IMRT dose-distribution measurements is still the ionization chamber. Although the ionization chamber does not directly measure the dose to water, the method for converting the measured quantity, ionization, to dose is well understood. There are limitations, however. Because an ionization chamber is an integrating dosimeter, the entire fluence distribution must be delivered for each measurement, yielding the dose at only a single point. Thus, the ionization chamber is an accurate, although inefficient, dosimeter for measuring IMRT dose distributions. The finite ionization chamber volume may lead to an inaccurate dose measurement as a result of volume-averaging of the dose distribution. Therefore, the size of the ionization chamber must be considered before its use. It is important that the chamber cross-section be smaller than the homogeneous dose regions in which it is placed. Also, the response should be determined as a function of incident beam angle when multiple beam angles are used. Low *et al.* (170) used a 0.125 cm<sup>3</sup> cylindrical ionization chamber with a cross-section of 6 × 5 mm<sup>2</sup> for measuring doses with the Nomos MIMiC serial tomotherapy MLC. The ionization chamber response was found to be within 1% of radiochromic film and a much smaller 0.009 cm<sup>3</sup> chamber, when the cylindrical chamber was well aligned with the 1.68-cm-thick tomotherapy slice field. However, the response deviated when the chamber was more than 2 mm from the slice center. Therefore, in such cases, it is essential that procedures be in place to ensure that the chamber position is known to better than 1 mm.

Thermoluminescent dosimeters (TLDs) have also been used for IMRT point dose measurements (10, 170). When properly calibrated, TLD chips provide an integrating dosimetric measurement capable of accuracy of better than 3%, with similar precision. The principal advantage of using TLD chips is the ability to simultaneously place dozens of chips in a phantom. With commercial automated TLD readers, the use of large numbers of TLD chips becomes practical. A commercial TLD sheet is also being produced that may be capable of measuring coarse 2D dose distributions.

Although single-point measurements provide useful in-

formation regarding the dose at selected points, they are impractical for providing 2D dose-distribution measurements. Ideally, a 2D dosimeter should be linear and water-equivalent. Radiochromic film conforms to these requirements, but the techniques required for accurate dose measurements have not been universally adopted, and the film still requires doses of  $\geq 20$  Gy. Radiographic film is not water-equivalent, and the precision of the film is strongly linked to the quality of the measurement and film processing techniques. However, radiographic film and processing equipment are universally available in RT departments. Therefore, it merits consideration for testing and periodic QA of IMRT dose distributions.

Considerations regarding the film sensitivity and other issues lead to the conclusion that it is quite difficult to use film as an absolute dosimeter and that it also requires significant effort to use as a precise relative dosimeter. One useful method based on film is to use it to localize the high-gradient regions in the distribution, because precise dose measurements are not required in regions of a high-dose gradient if the position of that gradient is all that is being measured. This task is precisely the task that is ill suited for point dosimeters like ion chambers. Although this does not guarantee that the dose distribution is correct everywhere, it does provide a useful QA tool.

A relatively new dosimeter, BANG (bis, acrylamide, nitrogen, and gelatin) gel, may prove useful for IMRT dose-distribution measurements (171). The dosimeter is a gelatinous medium that relies on the polymerization and cross-linking produced by ionizing radiation and subsequent increases in the solvent proton relaxation in the presence of the polymer. The increased proton relaxation rate ( $R_2 = 1/T_2$ ) can be imaged using MRI. The gel is irradiated using IMRT delivery and subsequently imaged using a clinical MRI unit.  $T_1$ - and  $T_2$ -weighted scans are obtained for each gel, and the volumetric distribution of  $R_2$  is determined using these scans. A monotonic relationship exists between  $R_2$  and the absorbed dose, but because the gel's radiation sensitivity is batch dependent, some gels must be irradiated to known doses and scanned to obtain a dose-calibration curve. A measurement of the full 3D dose distribution is provided by this method. Currently, cost, thermal sensitivity, and the requirement of MRI for readout limit the use of this detector medium to a few dosimetry studies. Research is being conducted on optical scanning of gel dosimeters with subsequent reconstruction to obtain the 3D dose distributions (172, 173).

In addition to the verification of IMRT dose distributions by measurement, Ma *et al.* (174) has reported on the use of Monte Carlo simulation as an independent check of the IMRT dose distribution.

#### IMRT treatment plan test cases

An essential component of thorough dosimetric verification is to study treatment plans and prescriptions that mimic the range of target volume and organ-at-risk geometries that will be used clinically. No complete set of IMRT plans has

yet been developed for testing purposes, but the CWG believes the treatment plans should exhibit the following characteristics:

A variety of target volume sizes and shapes should encompass the clinical range.

The sizes and shapes of organs at risk, as well as the geometric relationship among them, should be modeled from clinical cases.

The placement of targets should be varied to provide verification of the treatment planning and delivery systems throughout the available delivery and planning space.

Full 3D plans should be performed. It may also be useful to study 2D plans using coplanar beams to provide a study of the dose calculation and delivery in experiments that are relatively insensitive to spatial errors in the orthogonal direction, allowing for more accurate measurements. These measurements can help to distinguish between dose measurement and planning or delivery errors in more complex IMRT plans.

The treatment plan prescriptions used for testing purposes should provide regions of high-dose gradient such that the spatial localization accuracy can be determined in all three directions. This is particularly important if radiographic film is the only area dosimeter used.

Anthropomorphic phantoms can be used for verifying the IMRT dose distribution, as shown by Verellen *et al.* (11) and Low *et al.* (12). Plans verified using these phantoms inspire confidence because of their human geometry appearance. They are also useful to test certain features of the immobilization system. However, they have some drawbacks. Because they are inhomogeneous, the evaluation of dose-distribution accuracy may be more difficult, especially if a homogeneous dose-calculation algorithm is used. Care must be taken to determine the relative location of the dosimeters and external alignment marks. Many anthropomorphic phantoms do not have regularly spaced dosimeter locations, and a measurement of their locations relative to the external alignment marks is required. For patient QA, anthropomorphic phantoms are often not better models of the patient than regular geometric phantoms. For example, in the head and neck, the diameter of the patient at a particular location relative to the alignment system may vary dramatically as a function of head rotation; therefore, if the anthropomorphic phantom and patient head tilt are different, the diameter and, consequently the dose, to a measurement region may differ.

Although regular geometric phantoms do not look like patients, they have some very useful properties that enable the acquisition of accurate dose measurements. Regular geometric phantoms can be machined to tight spatial tolerances, and inserts for a variety of detectors can be fabricated for them. The relative location of the dosimeters and the phantom alignment marks (or other system) can be determined with a high degree of accuracy.

One feature that is important to have available in the IMRT planning system is the ability to apply the fluence

distribution designed for one treatment plan to the anatomy of another plan without fluence reoptimization. This is extremely important, because it allows the shift of a patient fluence distribution to a measurement phantom anatomy, thereby making routine patient dosimetric QA testing much easier. To help with the analysis of measured and calculated dose distributions, it is also useful to be able to register the two distributions. In addition, the ability to move the plan a predefined distance in all three dimensions (before calculating the dose distribution) allows the user to overlap the plan's high-dose and high-dose gradient regions with the dosimeters in a measurement phantom.

#### *QA checks of MU calculations*

Because of the complexity of IMRT delivery, IMRT treatment planning systems provide the MUs required to deliver each field. Therefore, an independent check of these MUs is required, but unlike traditional conformal beams, a straightforward manual calculation check is not possible. The MUs must be verified either by direct measurement or by an independent and validated calculation system (175, 176). The selection will depend on the availability of an independent calculation system.

Direct measurement involves the use of a phantom, either anthropomorphic or geometric, that is irradiated using the same accelerator MLC leaf sequences as the patient's treatment. The dose distribution within the phantom will not be the same as for the patient, so for highly accurate comparisons, a treatment plan computed using the phantom geometry with the patient's incident beam fluence is required.

Computational verification of MUs is a more efficient validation technique (158, 176–178). The computation model should consider effects of MLC leaf leakage, leaf transmission, radiation scatter, finite source geometry, leaf side and end transmission, and the effects of leaf sequencing. The verification of this algorithm and its implementation will require direct dose measurements, but the treatment plans and verification measurements can all be conducted in phantoms, enabling highly accurate comparisons. Validation and QA of MU verification software should be conducted in a similar manner to treatment planning software.

Although measurement-based verification tests both the MU determination and dose delivery, it is very manpower intensive. A systematic approach to validate the stability of the MU calculation may include the use of standard IMRT treatment plans. The plans could be verified by direct measurement and then rerun on a periodic basis to ensure that the treatment planning system data files have not been corrupted or altered. Once the accuracy and stability of the MU calculations have been established at a clinic, these plans may offer an efficient check of the IMRT treatment planning system, and specifically the MU calculations. Periodic measurement-based verification is still important to check the entire planning and delivery process.

#### *IMRT treatment verification*

Accurate delivery of IMRT treatments will depend on thorough accelerator and delivery system QA programs. A description of all linear accelerator QA procedures is beyond the scope of this paper, and the reader is referred to the AAPM reports addressing linear accelerator QA and safety issues (179, 180). We summarize only some of the specialized procedures specific to IMRT.

The accurate localization of the accelerator isocenter relative to the patient alignment fiducial markers is important for noninvasively immobilized patients. The origin within the patient is aligned to the accelerator using the positioning lasers. Dose delivery errors can occur because of excessive gantry sag, especially for serial tomotherapy IMRT (e.g., the Peacock system), and thus QA tests to check beam and isocenter alignment are essential.

For serial tomotherapy IMRT, accurate patient (table) positioning between arcs is extremely important. Low *et al.* (75, 181) determined that an incorrect placement of the patient between successive arc treatments can cause as much as 20%  $\text{mm}^{-1}$  dose heterogeneity in the abutment region. Consequently, the accuracy of the patient immobilization and placement system is critical to accurate dose delivery. Periodic testing of patient indexing system accuracy should be conducted.

The use of DMLC or SMLC-IMRT methods places unprecedented constraints on leaf position accuracy. LoSasso *et al.* (182) determined that for a 1-cm sliding window, an error of as small as 1 mm in the leaf opening yields a 10% error in delivered fluence. The traditional tolerance on MLC position calibration is 2 mm, as determined by the required precision of the portal edge positions. However, as shown by the LoSasso *et al.* (182), MLC position calibration errors introduce potentially significant dose delivery errors for IMRT. Additionally, studies by Low *et al.* (183) and Convery and Rosenbloom (78) have investigated variations in the delivered dose distribution when the gantry, collimator, or couch angle is incorrectly set. New QA procedures are required to monitor leaf position accuracy, and physicists will need to consider the influence of gravity and off-axis position, as well as dynamic delivery, for DMLC-IMRT.

As with all QA procedures, the relationship between procedure complexity and frequency must be balanced against the significance of undetected errors. Because the MLC leaf position calibration directly and significantly affects the delivered dose, a daily dosimetric check should be conducted when using dynamic delivery, which can be a simple modification of a daily output check. The same detector used for the daily photon output check can be irradiated by a DMLC-IMRT delivery of a homogeneous fluence distribution. Such a daily check may inspect only a few leaves, so a less frequent check (perhaps weekly) that inspects all leaves should be conducted. Chui *et al.* (184) have developed a straightforward film irradiation that is very sensitive to multileaf position calibration errors and offers a rapid visual inspection that can detect leaf errors as

small as 0.5 mm. If this test is conducted with the film placed at the level of the blocking or wedge trays, a single  $25.4 \times 30.5 \text{ cm}^2$  film may capture the entire  $40 \times 40 \text{ cm}^2$  available field area. This film test should be repeated at the four cardinal gantry angles.

Electronic portal imagers may also provide a very useful tool in the verification of DMLC or SMLC-IMRT (185, 186). Using this technology, it is feasible to capture leaves at particular intervals; more importantly, an integrated composite image could also be captured.

The verification of IMRT treatments represents a major challenge, and requires a shift from the conventional paradigm of weekly portal imaging. Although it is always possible to acquire an image with an adequately large portal to verify the patient's position, it seems meaningless to acquire a portal image of every IMRT field segment, because very little anatomic information is provided. The use of the images to verify beam weight would need to de-convolve the coupled patient variation—a very difficult problem. Indeed, in the proposed helical tomotherapy system by Mackie *et al.* (76), dose verification will be performed by reconstructing the delivered fluence with the patient 3D CT data, acquired at the time of treatment, as prerequisite input information.

In many centers that have clinically implemented IMRT, verification of machine output and patient positioning are treated as independent problems (10, 12, 187). In most instances, a pair of orthogonal open field images is acquired to verify patient setup before initiation of the delivery process. In other systems, the alignment of anatomy with the apertures of intensity-modulated fields is checked. For systems using DMLC techniques, the aperture of an intensity-modulated field is defined by the terminal position of the leading leaves and the starting position of the trailing leaves. Unlike the manual placement of a Cerrobend block or a beam modifier, the computer-control technology used for IMRT delivery provides much more assurance that the radiation machine will or has performed within its specifications, thereby allowing verification of patient setup to be performed independently. It follows that the ability to acquire patient images from projections other than that of the treatment beam will allow on-line verification of the patient during treatment. Such capability will certainly alleviate some of the difficulties associated with verifying a serial tomotherapy IMRT treatment using the MIMiC system.

Finally, treatment interruptions during IMRT delivery (i.e., machine failure during treatment) are a problem for most record and verification systems. Proper recovery of treatment interruptions should be tested as part of the acceptance testing and commissioning of the delivery system, and a written procedure addressing this problem must be in place.

*Recommendations: Acceptance testing, commissioning, and QA of IMRT systems and treatment verification*

The following list summarizes the recommendations regarding acceptance testing, commissioning, and QA for

IMRT planning and delivery systems and treatment verification for IMRT:

1. The accuracy (magnitude and position) of the IMRT dose distributions must be verified before clinical use of the IMRT system. Treatment planning companies are encouraged to implement dose-distribution measurement comparison software to enable a more thorough evaluation of the calculated dose distributions.
2. The commissioning process for an IMRT planning system should include the determination of the effects of the input parameters on the optimized dose distribution. This evaluation should be conducted using clinical patient scans and tumor volumes and should be completed for each treatment site.
3. The development of acceptance testing criteria and procedures for IMRT planning systems will be critical for the widespread clinical implementation of IMRT. Creating a standard set of phantoms with defined geometries (target volumes and critical structures) would help enable comparisons between different IMRT planning systems and develop criteria for acceptance testing and commissioning.
4. Dose measurements for testing IMRT systems must be conducted using non-uniform beam fluences, and the consequences of those fluences on dose measurements must be considered by the medical physicist.
  - Appropriate selection of detectors and the accurate determination of the detector spatial locations are critical to achieving accurate results.
  - The spatial relationship between the dosimeter and the phantom is required, as is the relationship between the accelerator alignment mechanism and the phantom.
  - The position of the calculated doses must be known. The IMRT planning system should be capable of providing the coordinates of the calculated doses.
5. Commissioning should include a thorough dosimetric verification of treatment plans and prescriptions that mimic the range of the clinical target and organs-at-risk geometries anticipated to be used clinically.
  - The treatment plan prescriptions used for testing purposes should provide regions of high-dose gradient such that the spatial localization accuracy can be determined in all three directions.
  - Anthropomorphic phantoms may be useful for verifying IMRT dose distributions. Care must be taken to determine the relative location of the dosimeters and external alignment marks. Geometric phantoms have the advantage that the relative location of the dosimeters and the phantom alignment marks can be determined with a high degree of accuracy.
  - The IMRT planning system should have the capability to apply the fluence distribution designed for one treatment plan to compute the dose to the anatomy of another plan without fluence reoptimization.

6. The MUs generated with the treatment-generated IMRT planning system must be independently checked before the patient's first treatment. Measurements can suffice for a check as long as fluence distributions can be re-computed in a phantom.
7. The verification of IMRT delivery requires a shift from the conventional paradigm of portal imaging. Verification of machine output and patient positioning may be treated as independent problems, at least initially.
8. Integrity of treatment machine mechanical movement and radiation output should be verified with special QA measures.

### FACILITY PLANNING AND RADIATION SAFETY

The principal facility shielding issue for IMRT is that significantly more machine beam-on time is required for IMRT techniques. Conventional RT treatments with non-IMRT fields generally encompass the entire planning target volume (PTV) with most fields, while IMRT techniques, using the equivalent number of machine MUs as the conventional treatment fraction, would deliver dose to only a part of the PTV. Therefore, depending on the complexity of the IMRT intensity pattern chosen, a potentially much larger number of additional MUs may be needed to cover the entire PTV. This increase in MUs has a serious consequence in two primary areas of concern, namely the recommended workload associated with the use of linear accelerators in shielding design (188, 189), and the increased whole-body dose to the patient that may occur because of increased leakage resulting from the large MU settings.

#### *Workload estimates*

It is important to specify the IMRT delivery system and the disease sites in trying to determine a useful value for the workload. For example, Grant (13) evaluated the workload for serial tomotherapy, using a MIMiC type collimator on a 10-MV X-ray accelerator treating a combination of cranial and head-and-neck cancer patients. Prescription doses ranged from 1.5 Gy/fraction to 2.4 Gy/fraction. The number of daily treatment arcs ranged from a minimum of 2 to a maximum of 5. The average MU setting/patient/d was 1426, and for 25 patients daily, the resulting workload was 178,250 R/wk at the isocenter. Similar data were obtained for a 15-MV X-ray accelerator treating only prostate cancer by way of serial tomotherapy to a prescription dose of 70 Gy in 35 fractions. The average MU setting was 1561 MU/patient, and for 25 patients daily, the resulting workload was 195,125 R/wk at the isocenter. This is significantly larger than the 100,000 R/wk at the isocenter recommended by the National Council on Radiation Protection and Measurements Report 49 (188) for 10-MV X-rays for the treatment of 50 patients. Although it may not be possible to put an absolute value on the recommended workload for all IMRT delivery systems and beam energies, it is clear that there is a large increase in the workload for IMRT that

requires consideration of the shielding design, particularly for the parts of the shielding calculation associated with leakage radiation. It is likely that for the present technology, one needs to increase the recommended values of workload from the National Council on Radiation Protection and Measurements Reports 49 and 51 (188, 189) by at least a factor of 2 and possibly as high as 5.

The increased workloads associated with IMRT can be represented by using a multiplicative factor,  $M$ , which is defined as the ratio of the number of MUs required for IMRT treatments divided by the number of MUs required when conventional-shaped fields are used. Followill *et al.* (190, 191) published a theoretical evaluation of the MU settings required to deliver IMRT with a SMLC technique and with serial tomotherapy (MIMiC). They looked at 6, 18, and 25-MV X-ray beams and compared the results with those for conventional therapy with and without wedges. After a review of multiple IMRT plans for several disease sites treated with SMLC-IMRT, they determined the ratio  $M$  to be 2.8. It is useful to note that this estimate is similar to the value arrived at by simply assuming the use of 60° wedges in each open field, because wedge factors for large-angle wedges can vary from 0.3 to 0.5, depending on the field size and manufacturer. It is clear, however, that the number of MUs used for SMLC or DMLC-IMRT techniques depends on the complexity of the IMRT intensity patterns used; for example, even the simple use of two sets of half-blocked fields to treat a single target volume effectively doubles the number of MUs used to treat a particular target. Therefore, the workload multiplier  $M$  must be estimated for the techniques to be used and cannot be assumed to be one particular value.

The workload multiplier  $M$  for serial tomotherapy is more complicated, because the treatment requires multiple arcs to deliver the dose to the entire volume. In the most simplistic terms, this would imply a serial tomotherapy IMRT treatment to have a ratio  $M$  larger than MLC-based IMRT systems by a factor of  $N$ , where  $N$  is the number of arcs (table indexes) needed to treat the entire volume. Followill *et al.* (190, 191) assigned  $M$  a value of 8 for MIMiC treatments on the basis of data for cranial treatments with the MIMiC used in the 1-cm slice length mode, which yielded a ratio  $M/N$  of 2.7/arc and an average of 3 arcs/patient. However, the ratio  $M/N$  and the total number of arcs vary with the disease site, as well as with the complexity of the treatment. In addition, they also depend on whether the MIMiC is used in the 1 or 2-cm slice length mode. Current data from the same institution that provided information for the Followill *et al.* study now indicate that the ratio  $M/N$  for cranial and head-and-neck cancer patients ranges from 2.0 to 2.2/arc, and the average number of arcs is 3 for cranial and 4 for head-and-neck cancer patients (192). For prostate treatments using 15-MV X-rays and the 2-cm slice length on the MIMiC, the  $M/N$  ratio for prostate treatment is 1.6/arc, and the average number of arcs is 3, yielding a value for  $M$  of 4.8. Mutic and Low (193) reported that for head-and-neck treatments with a 1-cm slice length for the

MIMiC, an average of 450 MUs/arc and 5 to 7 arcs are needed to deliver 2 Gy/fraction using 6-MV X-rays. Thus, these data yield an  $M/N$  ratio of 2.0/arc and a value for  $M$  ranging from 10 to 14.

#### *Dose rate and calibration changes*

Another basic machine factor is relevant to the shielding design issues discussed here. During the past decade, linear accelerator designs have improved so that much higher dose rates are available from many machines. Although the dose rates were typically limited to between 200 and 300 MU/min on many machines, manufacturers have provided machines that can treat patients with dose rates of 600 MU/min or higher (as much as 1000 MU/min in some modes). Driven by the desire to treat IMRT cases (requiring many MUs in shorter times), this dose rate improvement is expected to continue. Although older shielding regulations depended more on the total MU delivered than the dose rate, there are now states that consider the instantaneous dose rate as well. The new and higher dose rates must be considered for these situations.

A second effective increase in both workload and dose rate is the trend to calibrate modern accelerators at a depth of 10 cm. Before the past decade, it was clearly standard practice to calibrate most accelerators so that 1 machine MU delivered 1 cGy for a  $10 \times 10$ -cm field at source-surface distance (SSD) 100 cm at a depth of  $d_{\max}$  (1.5–3 cm) in water. However, in recent years, the concentration on CRT, increased knowledge of electron contamination and head scatter effects, and various other issues have led to the general acceptance (and even recommendation) of calibration at a depth of 10 cm. In such cases, 1 MU now corresponds to 1.0 cGy at a 10-cm depth, which translates to between 1.3 and 1.4 cGy at  $d_{\max}$ . This means that the effective dose rate delivered through the machine is a factor of 1.3 or 1.4 larger than before. Again, for those states that consider instantaneous dose rate also, this becomes a factor that must be considered.

#### *Shielding design*

The increase in MUs (ratio  $M$ ) for IMRT delivery clearly demonstrates that the workloads to be used to calculate the shielding requirements in room design are significantly different from those used for conventional therapy. One must take these numbers into account when looking at both primary and secondary barriers. The issues to be considered include angular distribution of primary radiation (i.e., gantry angle distribution), primary wall shielding, shielding for scatter, and shielding for leakage/transmission.

*Number of patients treated with IMRT.* The number of patients treated with IMRT is dramatically increasing every year. It is entirely conceivable that eventually most conformal and/or curative patients will be treated with some version of IMRT techniques. Therefore, the estimates of the percentage of patients treated with IMRT should range from 50% to almost 100%.

*Angle.* The angular distribution assumption for the field

directions should be uniform. As 3D-CRT has become a standard part of modern RT, the number of fields used per patient has increased and a more uniform distribution in gantry angle has become normal. For both MLC and MIMiC IMRT, most planning involves either arcs (MIMiC) or many nonopposed fields. The angular distribution of fields now has no significant concentration in AP-PA or four-field box directions.

*Primary barrier.* It appears safe to conclude that, in general, the total dose delivered to the patient will not change dramatically (factors of 2 or more), so it is unlikely that the primary barrier calculations for most facilities should change dramatically. In IMRT, each small area of the tumor is treated with the same dose, even though using “different” MUs. Thus, the primary barrier calculations need only consider the increase in dose rate, appropriate use factors, and calibration changes.

*Scatter.* Similar reasoning applies to the calculation of scatter: the same amount of radiation is delivered to the patient, so the same amount of scattered radiation will be spread around the treatment room. Probably no significant change in scatter calculation is required.

*Transmission/leakage.* Transmission/leakage is the part of the shielding calculation in which IMRT most dramatically changes the results of normal methods. The leakage issue is directly related to the MUs run through the machine. If the increase in MUs is a ratio of 5 from the normal workload, then all the parts of the shielding design that depend on leakage/transmission must be increased by a factor of 5. This is equivalent to the MU per week changing from 50,000 to 250,000 MU/wk or to increasing the leakage specification for a machine from 0.1% to 0.5%. Thus, treatment machine vendors are encouraged to add shielding in the head of the machine to avoid costly room shielding additions.

*Neutron dose.* For the high-energy (15 MV and higher) accelerators used for IMRT, neutron-shielding issues should also be considered. Because the number of neutrons produced by most machines scales linearly with the number of MUs run through the machine, the IMRT workload multiplier  $M$  should also be applied to neutron shielding calculations. This situation may require more neutron shielding.

#### *Patient whole-body dose*

The increase in workload for IMRT also increases the amount of leakage radiation in the treatment field and contributes to an increase in the whole-body burden outside the treated area. The estimates of the whole-body dose for varying kinds of IMRT are in basic agreement. Mutic and Low (193) reported the measured whole-body dose for serial tomotherapy from 6 MV X-rays (Clinac 6/100, Varian Corp.) for the head and neck to be approximately 300 mSv (~30 cGy) as opposed to the 543-mSv dose predicted by Followill *et al.* (190, 191). For a 10-MV X-ray beam (M74, Siemens Corp.) Grant *et al.* (194) measured the leakage dose as 520 mSv for serial tomotherapy, close to the Fol-

lowill *et al.* (190, 191) value for 6-MV X-rays but lower than their 2971 mSv calculated for 18-MV X-rays.

#### *Recommendations: Facility planning and radiation safety*

The following list summarizes the CWG recommendations regarding facility planning and radiation safety:

1. Increased workload values for IMRT (may be a factor of 2–5 larger than that for conventional therapy) should be considered mainly for the leakage/transmission part of the shielding calculation.
2. Differences between the measured data and theoretical estimates suggest that the actual leakage should be verified for various IMRT techniques, photon energies, and delivery systems.
3. Increased neutron production for high-energy machines used for IMRT should be considered.
4. Total-body dose for IMRT patients is higher, generally increasing with the number of MUs used for treatment. The potential for complications related to this increased dose should be recognized and considered in the implementation of IMRT.
5. Because IMRT is inherently less efficient (per MU) than conventional RT, vendors should consider the use of more internal shielding in the design of future IMRT machines.

### TARGET VOLUME AND DOSE SPECIFICATION AND REPORTING

The importance of providing a clear and unambiguous description of the RT when specifying a treatment regimen and reporting clinical results is obvious. Difficulties associated with dose and volume specification for conventional RT have been pointed out by several authors (195, 196). For example, is the reported dose the minimal dose to the target volume? Or is it the dose at or near the center of the target volume? The International Commission on Radiation Units and Measurements (ICRU) has addressed the issue of consistent volume and dose specification in RT, publishing ICRU Report 29 in 1978, ICRU Report 50 in 1993, and ICRU Report 62 in 1999 (197–199).

One of the important factors that has contributed to the success of the current 3D-RTP process is the standardization of nomenclature published in ICRU Report 50. This report has given the radiation oncology community a language and method for image-based 3D planning for defining the volumes of known tumor (gross tumor volume [GTV]), suspected microscopic spread (clinical target volume [CTV]), and marginal volumes necessary to account for setup variations and organ and patient motion (PTV).

The ICRU recently updated the recommendations of ICRU Report 50, but did not address the specific needs peculiar to IMRT (199). There appears to be a need for some modification in the ICRU recommendations.

#### *Target volume specification*

The clinical use of IMRT is generally motivated by the desire to conform the high-dose region to the target without inflicting unacceptable normal tissue complications. In general, the high-dose region is shaped to conform to the geometry of the target in three dimensions with rapid fall-off in all directions outside the target volume. Thus, the dose delivered to tissue outside the target volume can be significant if setup error or tumor motions are greater than the allowed treatment planning margins. In addition, because each IMRT segment treats only a portion of the target volume at a time, there may be significant dosimetric consequences if the patient and/or the target moves during treatment. Hence, it is clear that IMRT imposes a more stringent requirement than conventional RT in terms of accounting for patient position-related organ motion, interfraction organ motion, and intrafraction organ motion. All technical and clinical aspects of this part of the treatment planning process must be re-evaluated in light of this requirement.

*GTV and CTV.* Treatment planning, whether forward or inverse, can be a futile endeavor if the tumor volume is not correctly identified. As previously indicated, ICRU Report 50 identifies three different volumes that should be delineated (198). The GTV describes the part of the cancer that can be directly imaged or palpated. CT alone often fails to identify the GTV adequately or, more accurately, does not identify the same GTV as determined using other imaging studies (200, 201). MRI, various nuclear medicine studies, magnetic resonance spectroscopy, and even ultrasonography are in routine, but sporadic, use within the radiation oncology community. However, no guidelines exist to aid the clinician in knowing the conditions under which specific imaging modalities would be best used. This is an important area of research.

The delineation of the CTV depends heavily on *a priori* knowledge of the behavior of a given tumor. For a given GTV, tumor histologic features, and patient type, a set of probabilities exists that the tumor will, or will not, extend into a given regional organ or lymph node. However, these specific data are usually not available to the radiation oncologist—only general principles are known. More quantitative, consistent definition of CTVs is an important need.

*Planning target volume.* A critical point in the planning and delivery of IMRT is the prescription of meaningful PTVs for the patient. The PTVs must ensure proper coverage of the CTVs in the presence of the interfraction and intrafraction variation of treatment setup and organ motion. An inadequate PTV will typically lead to under dosing of the CTV and/or overdosing of the surrounding organs at risk. The conventional approach of creating a PTV by assigning a uniform margin around the CTV is no longer adequate for IMRT.

The complexity of IMRT necessitates the careful examination of whether a computer-optimized plan can be faithfully delivered to the patient. Conversely, one can ask whether a particular patient is a suitable candidate for IMRT

treatment. Recent in-depth studies based on daily electronic portal imaging and repeated CT scanning clearly demonstrate that uniform margin reduction, to the level required for dose escalation, cannot accommodate the variation of treatment setup and organ motion (202). On the other hand, such studies improve our understanding of treatment uncertainty and allow the development of new approaches for more appropriate PTV prescription (203).

For each patient, there are two components to the geometric uncertainty: setup variation and organ motion. A first-order approach is to treat them independently, although in several instances, they have compounding effects on each other. Both setup and motion must be considered to accommodate the inter- and intrafraction treatment variation. Efforts have also been made to further model the variation into its systematic and random components.

For the daily setup variation, the systematic component is often larger than the random component (204). It follows that with the conventional approach of prescribing the PTV, according to an institutional standard, much of the PTV margin used is needed to accommodate interpatient variation. A substantial margin reduction can be attained by correcting the systematic component such that only random setup variation needs to be accounted for by the PTV. This inherently individualized approach requires more frequent portal imaging for determining the systematic and random components of the setup variation. Although the approach does require increased efforts from all treatment personnel, several clinical models have been successfully and efficiently implemented (204). Furthermore, recent experience suggests that, with a properly implemented network infrastructure that accommodates electronic portal imaging, the process imposes minor, if not a smaller, burden on the personnel than the present practice with weekly port film imaging. As for the intrafraction setup stability, very few systematic studies have been done to evaluate its magnitude. It is often assumed to be insignificant in conventional treatment. This assumption needs to be re-examined for IMRT because of the extended treatment time.

The study of PTV-organ motion has been mainly directed to the problems of interfraction variation in the treatment of prostate cancer and the intrafraction variation of breathing motion for disease in the thoracic and upper abdominal regions. Several radiographic and CT studies have shown that the prostate position can vary by  $>10$  mm between treatment fractions and that the variation in rectal position exhibits a time-trend dependence with the course of treatment (202).

Some uses of IMRT are predicated on the desire to escalate the tumor dose delivered to the patient. To accomplish this goal, it may be helpful if the margin for the PTV can be reduced further with more direct treatment intervention. The Adaptive Radiation Therapy paradigm described by Yan *et al.* (205) uses early measurements during patient treatments to more appropriately prescribe the required margins for later treatments based on the localization data for the individual patient.

A second method for improving the geometrical accuracy is a “target of the day” approach, which relies on image guidance in which the target position is identified daily (206). This can be performed with various imaging procedures such as ultrasound imaging, radiographic imaging of implanted radiopaque markers, or tomographic (CT) imaging. The general principle is to adjust the field to the daily position of the target as detected by each imaging procedure. Radiographic-guided delivery has been implemented for the head-and-neck region without implanted radiopaque markers, where the rigid body model of treatment variation may be valid. The overall PTV margin can be as small as a few millimeters. Ultrasound imaging has been adapted for IMRT prostate treatment localization at several institutes (207, 208). It should be noted that with radiographic or ultrasound guidance, a new patient reference point in relation to the treatment machine isocenter is calculated daily. Because the adjustment of the field position does not account for possible shape changes, and there are more residual errors in the process, a residual margin needs to be prescribed. Early reports on ultrasound-guided delivery suggest that the margin for PTV-organ motion can be reduced to about 5 mm (207). The tomographic guidance method is theoretically the most comprehensive of the three approaches, because the correction would account for both nonrigid soft tissue variation and daily setup error.

Both adaptive and image-guided delivery of IMRT may substantially increase the demand on the resources of the clinic, but may be necessary when the dose is escalated beyond normal ranges. The adaptive approach transfers the necessary effort off-line to preserve daily treatment efficiency. The image-guided approach is conceptually more powerful, but at the cost of additional daily effort. A third approach to reduce organ motion is through improved immobilization. For example, this has been accomplished for prostate cancer treatment by inflating a balloon in the rectum during the delivery of the IMRT (209).

A modest reduction in the size of the margin allowed for organ motion has been attained by using CT scans acquired near the end of the normal breathing cycle for planning (210). More recently, active intervention in ventilatory motion has been investigated, including the use of ventilatory-based gating (211), breath-holding (212), and active breathing control (213). The different methods include various tradeoffs, ranging from machine control, which is not dependent on the patient, to systems that are completely dependent on the patient; all require continued research before they are routinely available for clinical use. The choice of approaches to reduce the PTV for breathing motion is dependent (at least partly) on the IMRT delivery technique. The discrete nature of the SMLC method may be amenable to all three methods listed above. However, for delivery with the DMLC or tomotherapy methods, the breath-hold methods might be more suitable because gating requires additional control of the coupled mechanical motion.

### Dose specification

Specification of the doses used for both prescription and reporting is difficult for the fast-changing and non-uniform dose distributions often found when IMRT is used, and the specification is a problem that needs much new work. The ICRU recommendations regarding dose reporting for traditional 3D-CRT include the dose at or near the center of the PTV, as well as the maximal and minimal dose to the PTV (198). ICRU also recommends that any additional information such as the mean dose and the DVHs be reported when available. No firm recommendations regarding dose prescription have been provided.

The Nordic Association of Clinical Physics has proposed that for relatively small dose non-uniformity, the mean dose and its standard deviation to the CTV (with margin for internal motion) be used for both treatment prescription and reporting (214). When the relative standard deviation of the dose distribution is larger than the tolerance range (for steeply responding tumors and normal tissues, a relative standard deviation  $<2.5\%$ , and for more shallow responding tumors and normal tissues, a relative standard deviation of no more than  $5\%$ ), the Nordic Association of Clinical Physics recommends that the minimal dose to the CTV and mean dose delivered to the hot and cold volumes within the CTV be reported. Note, the Nordic Association of Clinical Physics defines the hot volume as a volume that receives a dose larger than the prescribed dose by an amount larger than the tolerance limit. A cold volume is defined as a volume inside the CTV that receives a dose lower than the prescribed dose to the CTV by an amount larger than the tolerance limit.

It should be pointed out that significant problems are associated with dose reporting of the maximal and/or minimal doses. For example, the minimal dose is highly uncertain because of uncertainties in the placement of the region of interest near high-gradient regions. The maximal dose is also unreliable, because it corresponds to the high-dose tail of the DVH. In both cases, the values depend on the voxel size. Also, with the advent in the future of Monte Carlo-based treatment planning, the maximal and minimal doses in a region of interest will be, by definition, several standard deviations away from the true maximal or minimal doses.

Niemierko (122) has introduced a new concept for summarizing and reporting inhomogeneous dose distributions called the *equivalent uniform dose*. This concept assumes that any two dose distributions are equivalent if they cause the same radiobiologic effect. McGary *et al.* (215) pointed out that there are conditions in which the equivalent uniform dose is not adequate as a single parameter to report or analyze inhomogeneous dose distributions (e.g., when the minimal dose is significantly lower than the mean dose) (216).

It is likely that to make possible quantitative use of clinical results involving IMRT, the entire DVH for each of the pertinent volumes (PTV, CTV, and the organs at risk) will need to be reported. Therefore, the CWG believes that the dose-volume data available directly from the DVHs generated by IMRT planning systems are more suitable for

correlating with clinical outcomes. The CWG suggests that, as a minimum, the dose that covers 95% ( $D_{95}$ ) and 100% ( $D_{100}$ ) of both the CTV and the PTV and the percentage of the CTV and PTV receiving the prescribed dose ( $V_{100}$ ) be obtained from a DVH and reported. The mean, minimal, and maximal doses (averaged over the nearest neighbor voxels) to each CTV and PTV should also be reported. Similarly, for the organs at risk, the mean, minimal, and maximal doses and other relevant dose-volume data should be reported.

### Recommendations: Target volume and dose specification

The following list summarizes the CWG's recommendations regarding target volume and dose specification for IMRT for the purposes of correlating them with the clinical outcome:

1. Clinicians should specify the target volume(s) following the recommendations of ICRU Reports 50 and 62 (198, 199).
2. The PTV must (at least attempt to) ensure proper coverage of the CTV in the presence of the inter- and intrafraction variation of treatment setup and organ motion. The conventional approach of assigning a uniform margin around the CTV is generally no longer adequate when IMRT plans are considered.
3. Application of IMRT to sites that are susceptible to breathing motion should be limited until proper accommodation of motion uncertainties is included.
4. Important research issues in the area of target volume specification include the following:
  - Development of guidelines defining which specific imaging modalities should be used for GTV delineation for specific sites.
  - Development of more automatic and robust methods of image registration suitable for routine use in RT treatment planning.
  - Development of quantitative methods and rules for CTV delineation.
  - Development of methods and/or technology to better account for and reduce spatial uncertainties.
5. As a minimum, the following information should be reported for the purpose of correlating the dose with the clinical outcome:
  - Prescribed (intended) dose, as well as the point or volume to which it is prescribed; a fractionation prescription should also be included.
  - Dose that covers 95% ( $D_{95}$ ) of the PTV and CTV.
  - Dose that covers 100% ( $D_{100}$ ) of the PTV and CTV (i.e., the minimal dose).
  - Mean and maximal doses within the PTV and CTV.
  - Percentage of the PTV and CTV that received the prescribed dose ( $V_{100}$ ).
  - For each organ at risk, the maximal, minimal, and mean doses, the volume of the organ receiving that dose, and other relevant dose-volume data.

## CLINICAL EXPERIENCE, CHALLENGES, AND CONTROVERSIES

The preceding sections addressed the major technical issues involved in the implementation of an IMRT program. Many of these issues are of practical clinical value to clinicians involved in the use of IMRT, and an additional discussion of these points from a clinical standpoint is warranted. Familiarization with the major kinds of IMRT and the associated jargon will allow all of us, physicians, physicists, dosimetrists, and others, to communicate with each other more effectively. Understanding the arguments concerning when treatment is “3D-CRT” and when it is “IMRT” should allow physicians to honestly answer questions about what is being offered to a patient and why. Finally, in the absence of prospective randomized trials, it is important to consider in what clinical setting (and with what techniques) we should expect the largest benefits with IMRT.

### *Clinical Experience with IMRT*

The published clinical reports on the use of IMRT for patient treatment fall into three general categories in this rapidly evolving field. The first category includes investigations into the potential benefits of IMRT treatment planning and delivery technology, typically studied with treatment planning comparisons involving one or more cases. A second set of publications deals with dosimetric confirmation of clinical IMRT treatment techniques, and a third includes clinical studies that report on a relatively small number of patients treated with IMRT techniques. Unfortunately, as of yet, no reports of prospective randomized clinical studies involving IMRT have been published, and this lack of information clearly limits our knowledge of how clinical outcomes are affected by the use of IMRT.

A number of authors have performed treatment planning comparisons between IMRT plans and other more standard plan types. Verhey and colleagues (217) have presented a comparison of conformal and different IMRT techniques on 3 patients (prostate, nasopharynx, and paraspinal), showing that the inverse-planned IMRT techniques can yield significantly better dose results, in some situations at the expense of additional time and resources for the IMRT plans. Lomax *et al.* (218) compared proton planning and photon IMRT planning for 9 patients with a variety of treatment sites. This work showed that the medium-to-low dose load for the proton plans was reduced compared with that for the photon plans and accomplished approximately the same kind of target conformation; however, this comparison was limited in that the proton plans were not performed using inverse planning (as the IMRT plans were). Hong *et al.* (219) reported on a treatment planning study that compared IMRT and standard tangential beam irradiation for 10 patients with breast cancer and showed that IMRT may improve uniformity within the breast tissue, while

also reducing the dose to the normal tissues, including the heart and lung. However, respiration and other important factors were not included in this study. Pickett *et al.* (220) reported on a single patient treatment planning study that demonstrated the feasibility of using IMRT to treat a dominant intraprostatic lesion (defined by endorectal MRI and magnetic resonance spectroscopy) to 90 Gy while not exceeding normal tissue tolerances. These investigators also demonstrated that different types of IMRT could be used to accomplish this feat. In a follow-up study, these investigators also demonstrated that this SMLC-IMRT technique is reasonably well tolerated on the basis of an analysis of patients who received >82 Gy to a portion of their prostate (221).

Khoo *et al.* (222) compared standard radiosurgery plans for 5 patients with IMRT plans generated using the Peacock system and found slightly improved PTV coverage, as well as somewhat higher organ-at-risk doses, for the IMRT plans. Cardinale *et al.* (223) compared radiosurgery and IMRT plans for a single patient with simulated target volumes and concluded that the IMRT plans appear to improve conformity and decrease the dose to nontarget brain tissue compared with standard radiosurgery arcs or six-beam conformal fixed-field treatment plans.

Dosimetric and localization studies for the clinical application of IMRT have also been published. Tsai *et al.* (224) reported on the dosimetric verification of 94 patients treated with sequential tomotherapy IMRT. Targeted diseases included, among others, glioma, astrocytoma, meningioma, brain metastasis, craniopharyngioma, nasopharyngeal cancer, lymphoma, melanoma, and prostate and esophageal carcinoma. This report on QA procedures concluded that over the course of the treatment of these patients they were able to reduce their QA efforts from individual per-patient procedures to more routine machine-specific QA. Verellen *et al.* (225) published a detailed description of the procedures used for the treatment of patients with head-and-neck tumors that received serial tomotherapy IMRT. Dose verification studies with alanine detectors, thermoluminescent dosimetry, and film dosimetry were conducted. The accuracy of patient positioning was within 0.3 cm and 2.0°, except in 2 cases, and the authors concluded that their noninvasive fixation technique was acceptable for treatment of these patients. However, they concluded that daily monitoring was mandatory if accuracy better than 0.1 cm and 1.0° was required for patient setup. Low *et al.* (12) reported on the clinical QA procedures for the treatment of head-and-neck cancer patients with serial tomotherapy describing the use of an ion chamber, TLD, and film dosimetry to confirm the plan accuracy. Ling *et al.* (14) and Burman *et al.* (187) provided a detailed description of their treatment planning, treatment delivery, and QA procedures for the treatment of patients with prostate cancer using DMLC-IMRT. These reports concluded that for complex planning problems in which the surrounding organs at risk placed severe constraints on the prescription dose,

Table 2. Conformal therapy techniques

Type of conformal therapy	Minimal dose calculation requirements	Minimal imaging requirements	Treatment delivery requirements	Degree of conformity*
Conventional 3DCRT	3D with DVHs	Full set of CT or MRI images	Cerrobend blocks or MLC	2
Forward-planned SMLC-IMRT	3D with DVHs	Full set of CT or MRI images	Computer-controlled MLC	3
Inverse-planned SMLC-IMRT	3D with DVHs	Full set of CT or MRI images	Computer-controlled MLC	2-4
DMLC-IMRT	3D with DVHs	Full set of CT or MRI images	Dynamic MLC	2-4
Tomotherapy IMRT	3D with DVHs	Full set of CT or MRI images	Tomotherapy device or at least linear accelerator with binary MLC	2-4

\* Conformality was subjectively rated on a scale of 1 to 5 (higher number indicating a higher degree of conformity) to point out to the reader that inverse-planned IMRT can be either better or worse than forward-planned techniques depending on the objective function and/or the input parameters used in the inverse planning process and on technical details related to the various delivery techniques. Note that no attempt was made to distinguish how well the three inverse-planned IMRT methods would compare against each other.

*Abbreviations:* 3D = three-dimensional; CRT = conformal radiotherapy; DVH = dose-volume histogram; MLC = multileaf collimator; SMLC = segmental MLC; IMRT = intensity-modulated radiotherapy; DMLC = dynamic MLC.

IMRT provides a powerful and efficient solution. A recent study by Fraass *et al.* (15) on the effect of computer-controlled treatment delivery on treatment delivery errors involved a large number of patients treated with SMLC-IMRT.

Several recent published reports have emphasized clinical end points in patients treated with IMRT. De Neve *et al.* (16) used an SMLC-IMRT technique to treat patients with head and neck or thyroid cancer. Doses of 70–80 Gy were delivered to the primary tumor volume without exceeding the tolerance of the spinal cord (50 Gy at the highest voxel). The in-target dose inhomogeneity was approximately 25%. The shortest time of execution of treatment (22 segments) on a patient was 25 min. De Neve *et al.* (226) also documented the successful repeated treatment of patients with pharyngeal cancer using their SMLC-IMRT techniques. Fraass *et al.* reported on the treatment of >350 patients using a somewhat different type of SMLC-IMRT. In this work, patients with a wide variety of clinical treatment sites were treated, including patients in dose-escalation studies of the brain, lung, and liver treated to doses of  $\geq 90$  Gy. Planning techniques, clinical treatment times, and plan optimization issues were described. Eisbruch *et al.* (227) reported on a parotid-sparing SMLC-IMRT technique of the head-and-neck region and demonstrated significant sparing of the parotid gland. Burman *et al.* (187) described a DMLC-IMRT technique used to treat 8 prostate patients and the extensive QA checks used.

Serial tomotherapy treatments have been described by a number of authors. Tsai *et al.* (10) provided a description of their treatment process using this technology for >92 patients. That report was followed by one documenting their serial tomotherapy-IMRT verification techniques used for the initial 12 patients (224). Kupper-Smith *et al.* (228) recently published a retrospective review of clinical treatment results for 28 head-and-neck

cancers patients who were treated using serial tomotherapy-IMRT. The authors reported significantly lower acute toxicity than was previously seen with conventional RT. Butler *et al.* (229) reported on their initial experience (20 patients) in the definitive treatment of head-and-neck carcinoma using a serial tomotherapy-IMRT technique they called simultaneous modulated accelerated radiation therapy (SMART). They reported that the initial tumor response was encouraging and the short-term toxicity acceptable. A larger patient population and longer follow-up are needed to evaluate the ultimate tumor control and late toxicity. Grant (13) and Grant and Cain (230) described the serial tomotherapy-IMRT technique used to treat >300 patients and concentrated on describing the procedures used for these treatments.

*SMLC, DMLC, or tomotherapy: What kind of IMRT should I use?*

Which kind of IMRT should be used in varying situations is a very common question during discussions of the clinical uses of IMRT. Table 2 summarizes the spectrum of 3D-CRT/IMRT techniques commonly available. SMLC-IMRT evolved directly from 3D-CRT. At institutions with an established program using 3D-CRT, the transition to SMLC-IMRT represents a very natural step toward more a sophisticated form of CRT. SMLC-IMRT, based on the use of multiple MLC shapes at a fixed gantry position, can be implemented using either forward or inverse planning, or with a combination of the two planning approaches. Without some forward planning, it is very difficult to be realistic about “where to start” in developing an optimized inverse plan, and without inverse planning, one can not be certain that other reasonable options would not yield a better result. SMLC-IMRT involving some forward planning has been in clinical use at centers in the United States and Europe

since at least 1994 (15, 16, 133, 220, 231). The last three rows of Table 2 list the IMRT techniques developed with inverse planning only. The quality of the CRT delivered with these techniques depends generally on the cost function used in the inverse planning process and on technical details related to the various delivery techniques.

#### *Advantages and disadvantages of various types of IMRT*

Each of these forms of IMRT have theoretical advantages and disadvantages. Forward-planned SMLC represents the least expensive and least complicated approach for taking CRT to the next level. Additional benefits of SMLC-IMRT include that films more closely resembling conventional port and simulation films can be generated, and that SMLC can make use of more intuitive forward planning approaches in certain situations. In contrast, inverse-planned IMRT (SMLC, DMLC, and tomotherapy) generally does not allow port films that closely resemble conventional port films to be generated. Nor do these methods allow clinicians to easily translate “what they would usually do” directly into an IMRT plan. DMLC and tomotherapy are often described as being capable of generating more conformal dose distributions than SMLC, although this has not been conclusively shown. These types of IMRT are likely to be of greatest value when the day-to-day setup variation and organ movement are minimized and when a very high dose is desired immediately adjacent to a critical structure. Both of these approaches require sophisticated inverse planning algorithms, which may reduce the dependence of the treatment planning process on the planning skills and experience of the dosimetrist (although significant skills are necessary to develop the cost function used by the inverse planning algorithm). Theoretically, inverse planning can be accomplished by setting the parameters and walking away to complete other tasks. Unfortunately, exactly just how these treatment parameters should be set for a given case often still involves a great deal of trial and error.

Several unique features suggest that in the future helical tomotherapy may hold great promise. First, if the tomotherapy device includes acquisition of CT images acquired in near “real-time,” it may be possible to account for organ movement and day-to-day setup variations, potentially performing adaptive RT (discussed in a previous section) (205). Adaptive RT involves modifying what was actually delivered immediately or before the time of the next treatment session. A disadvantage of the helical tomotherapy system is that it would require the radiation oncology department to purchase a new piece of equipment, with considerable initial costs. It remains to be determined just how this developing technique will compare with IMRT techniques, which make use of conventional computer-controlled, MLC-equipped linear accelerators.

#### *Clinical summary*

Thus, we see that no definitive studies have conclusively demonstrated the impact of IMRT on improved tumor con-

trol and decreased long-term morbidity, nor have any studies demonstrated the superiority of one particular IMRT technique—at least on a clinical basis. Ultimately, the value of IMRT needs to be tested to show that the use of IMRT will further the 3D hypothesis, as advocated by Lichter (232); that is, that 3D-CRT will allow higher doses of radiation to be delivered with equal or less morbidity than standard techniques. The IMRT CWG does not advocate the direct testing of IMRT vs. no IMRT—that would be too reductionist—nor, even, necessarily 3D vs. 2D planning. Rather, we advocate the testing of the high doses made possible by IMRT vs. conventional doses. The areas of interest include cranial, head and neck, lung, breast, pancreas, prostate, and gynecologic applications.

## CONCLUSION

IMRT is an advanced form of external beam irradiation often used to perform 3D-CRT. It represents one of the most important technical advances in RT since the advent of the medical linear accelerator. Currently, most IMRT approaches increase the time and effort required by physicians and physicists, because optimization systems are not yet robust enough to provide automated solutions for all disease sites, and routine QA testing is still quite time intensive. Considerable research is needed to model clinical outcomes to allow truly automated solutions.

Current IMRT delivery systems are essentially first-generation systems, and no single method stands out as the ultimate solution. In addition, IMRT techniques appear to place greater stress on the treatment machines. Currently, no articles about the effects of IMRT use on machine reliability, downtime, and failure rate have been published. This could become a potential issue in the future.

The instrumentation and methods used for IMRT QA procedures and testing are not yet well established. In addition, many fundamental questions regarding IMRT are still unanswered, including the radiobiologic consequences of altered time-dose-fractionation and that the dose heterogeneity for both the target and normal tissues may be much greater with IMRT compared with traditional RT techniques.

All that said, this new process of planning and treatment delivery shows significant potential for improving the therapeutic ratio. Also, although inefficient today, it is expected that IMRT, when fully developed, will improve the efficiency with which external beam RT can be planned and delivered, and thus potentially lower costs.

The recommendations contained in this report are intended to be both technical and advisory, but the ultimate responsibility for the clinical decisions pertaining to the implementation and use of IMRT rests with the radiation oncologist and radiation oncology physicist. It should be well understood that this is an evolving field, and the CWG expects modifications of these recommendations as new technology and data become available.

## REFERENCES

- Purdy JA, Starkschall G. A practical guide to 3-D planning and conformal radiation therapy. Madison, WI: Advanced Medical Publishing; 1999.
- Webb S. The physics of conformal radiotherapy. Bristol: Institute of Physics Publishing; 1997.
- Mackie TR. Radiation therapy treatment optimization. *Semin Radiat Oncol* 1999;9:1-118 (entire volume).
- Sternick ES, ed. The theory and practice of intensity modulated radiation therapy. Madison, WI: Advanced Medical Publishing; 1997.
- Webb S. Intensity-modulated radiation therapy. Bristol: Institute of Physics Publishing; 2000.
- Brahme A. Optimization of radiation therapy. *Int J Radiat Oncol Biol Phys* 1994;28:785-787.
- Carol MP, Targovnik H, Smith D, et al. 3-D planning and delivery system for optimized conformal therapy (abstract). *Int J Radiat Oncol Biol Phys* 1992;24:158.
- Fraass BA, McShan CL, Kessler ML. Computer-controlled treatment delivery. *Semin Radiat Oncol* 1995;5:77-85.
- Webb S. The physics of three-dimensional radiation therapy. Bristol: Institute of Physics Publishing; 1993.
- Tsai J-S, Wazer DE, Ling MN, et al. Dosimetric verification of the dynamic intensity-modulated radiation therapy of 92 patients. *Int J Radiat Oncol Biol Phys* 1998;40:1213-1230.
- Verellen D, Linthou N, Van Den Berge D, et al. Initial experience with intensity-modulated conformal radiation therapy for treatment of the head and neck region. *Int J Radiat Oncol Biol Phys* 1997;39:99-114.
- Low DA, Chao KC, Mutic S, et al. Quality assurance of serial tomotherapy for head and neck patient treatments. *Int J Radiat Oncol Biol Phys* 1998;42:681-692.
- Grant W III. Experience with intensity modulated beam delivery. In: Palta J, Mackie TR, editors. Teletherapy: Present and future. College Park, MD: Advanced Medical Publishing; 1996. p. 793-804.
- Ling CC, Burman C, Chui CS, et al. Conformal radiation treatment of prostate cancer using inversely-planned intensity modulated photon beams produced with dynamic multileaf collimation. *Int J Radiat Oncol Biol Phys* 1996;35:721-730.
- Fraass BA, Kessler ML, McShan DL, et al. Optimization and clinical use of multisegment IMRT for high dose conformal therapy. *Semin Radiat Oncol* 1999;9:60-77.
- De Neve W, De Wagter C, De Jaeger K, et al. Planning and delivering high doses to targets surrounding the spinal cord at the lower neck and upper mediastinal levels: Static beam-segmentation technique executed with a multileaf collimator. *Radiation Oncol* 1996;40:271-279.
- De Wagter C, Colle CO, Fortan LG, et al. 3D conformal intensity-modulated radiotherapy planning: Interactive optimization by constrained matrix inversion. *Radiation Oncol* 1998;47:69-76.
- Tsien KC. The application of automatic computing machines to radiation treatment planning. *Br J Radiol* 1955;28:432-439.
- Holmes WF. External beam treatment-planning with the programmed console. *Radiology* 1970;94:391-400.
- Bentley RE, Milan J. An interactive digital computer system for radiotherapy treatment planning. *Br J Radiol* 1971;44:826-833.
- Sterling TD, Perry H, Katz L. Automation of radiation treatment planning V. Calculation and visualisation of the total treatment volume. *Br J Radiol* 1965;38:906-913.
- Sterling TD, Knowlton KC, Weinkam JJ, et al. Dynamic display of radiotherapy plans using computer-produced films. *Radiology* 1973;107:689-691.
- van de Geijn J. The computation of two and three dimensional dose distributions in cobalt-60 teletherapy. *Br J Radiol* 1965;38:369-377.
- van de Geijn J. A computer program for three-dimensional planning in external-beam radiation therapy, EXTDOSE. *Comput Prog Biomed* 1970;1:45-57.
- Cunningham JR. Scatter-air ratios. *Phys Med Biol* 1972;17:42-51.
- Beaudoin L. Analytical approach to the solution of dosimetry in heterogeneous media [Ph.D. Thesis]. Toronto, Ontario: University of Toronto; 1968.
- Sontag MR, Cunningham JR. The equivalent tissue-air ratio needed for making absorbed dose calculations in a heterogeneous medium. *Radiology* 1978;129:787-794.
- Reinstein LE, McShan D, Webber BM, et al. A computer-assisted three-dimensional treatment planning system. *Radiology* 1978;127:259-264.
- McShan DL, Silverman A, Lanza D, et al. A computerized three-dimensional treatment planning system utilizing interactive color graphics. *Br J Radiol* 1979;52:478-481.
- Goitein M. Applications of computed tomography in radiotherapy treatment planning. In: Orton CG, editor. Progress in medical radiation physics. New York: Plenum Publishing; 1982. p. 195-293.
- Ling CC, Rogers CC, Morton RJ, eds. Computed tomography in radiation therapy. New York: Raven Press; 1983.
- Goitein M, Abrams M. Multi-dimensional treatment planning: I. Delineation of anatomy. *Int J Radiat Oncol Biol Phys* 1983;9:777-787.
- Goitein M, Abrams M, Rowell D, et al. Multi-dimensional treatment planning: II. Beam's eye view, back projection, and projection through CT sections. *Int J Radiat Oncol Biol Phys* 1983;9:789-797.
- Fraass BA, McShan DL. 3-D treatment planning. I. Overview of a clinical planning system. Proceedings of the 9th International Conference on the Use of Computers in Radiation Therapy, Scheveningen, The Netherlands, 1987.
- Purdy JA, Wong JW, Harms WB, et al. Three dimensional radiation treatment planning system. Proceedings of the 9th International Conference on the Use of Computers in Radiation Therapy, Scheveningen, The Netherlands, 1987.
- Sherouse GW, Mosher CE, Novins K, et al. Virtual simulation: Concept and implementation. Proceedings of the 9th International Conference on the Use of Computers in Radiation Therapy, Scheveningen, The Netherlands, 1987.
- Mohan R, Barest G, Brewster IJ, et al. A comprehensive three-dimensional radiation treatment planning system. *Int J Radiat Oncol Biol Phys* 1988;15:481-495.
- Smith AF, Purdy JA. Editors' note. *Int J Radiat Oncol Biol Phys* 1991;21:1.
- Austin-Seymour MM, George MD, Chen GTY, et al. Dose volume histogram analysis of liver radiation tolerance. *Int J Radiat Oncol Biol Phys* 1986;12:31-35.
- Drzymala RE, Holman MD, Yan D, et al. Integrated software tools for the evaluation of radiotherapy treatment plans. *Int J Radiat Oncol Biol Phys* 1994;30:909-919.
- Lyman JT. Complication probability as assessed from dose volume histograms. *Radiat Res* 1985;104:S13-S19.
- Lyman JT, Wolbarst AB. Optimization of radiation therapy. III. A method of assessing complication probabilities from dose-volume histograms. *Int J Radiat Oncol Biol Phys* 1987;13:103-109.
- Smith AR, Purdy JA, eds. Three-dimensional photon treatment planning. Report of the Collaborative Working Group on the Evaluation of Treatment Planning for External Photon

- Beam Radiotherapy. *Int J Radiat Oncol Biol Phys* 1991;21:3–268 (entire volume).
44. Smith AR, Ling CC, eds. Implementation of three dimensional conformal radiotherapy. *Int J Radiat Oncol Biol Phys* 1995;33:779–976 (entire volume).
  45. Computer Aided Radiotherapy News. Nordic R&D Program on Computer Aided Radiotherapy 1987; No. 5, April.
  46. Takahashi S. Conformation radiotherapy: Rotation techniques as applied to radiography and radiotherapy of cancer. *Acta Radiol Suppl* 1965;242:1–42.
  47. Proimos BS. Synchronous field shaping in rotational megavoltage therapy. *Radiology* 1960;74:753–757.
  48. Wright KA, Proimos BS, Trump JG, *et al.* Field shaping and selective protection in megavoltage therapy. *Radiology* 1959;72:101.
  49. Trump JG, Wright KA, Smedal MI, *et al.* Synchronous field shaping and protection in 2-million-volt rotational therapy. *Radiology* 1961;76:275.
  50. Green A. Tracking cobalt project. *Nature* 1965;207:1311.
  51. Jennings WA, Green A. The tracking cobalt-60 method, or programmed 3D irradiation. In: Abstracts of the Second Congress of the European Association of Radiology, 1971. Amsterdam: Excerpta Medica; 1971. p. 154.
  52. Green A, Jennings WA, Christie HM. Radiotherapy by tracking the spread of disease. In: Blickman JR, editor. Transactions of the Ninth International Congress of Radiology. Munchen: Verlag; 1960. p. 766–772.
  53. Davy TJ, Brace JA. Dynamic 3-D treatment using a computer-controlled cobalt unit. *Br J Radiol* 1979;53:612–616.
  54. Brace JA. A computer-controlled tele-cobalt unit. *Int J Radiat Oncol Biol Phys* 1982;8:2011–2013.
  55. Bjarngard B, Kijewski P, Pashby C. Description of a computer-controlled machine. *Int J Radiat Oncol Biol Phys* 1977;2:142.
  56. Brahme A. Design principles and clinical possibilities with a new generation of radiation therapy equipment: A review. *Acta Oncol* 1987;26:403–412.
  57. Brahme A. Optimization of conformation and general moving beam radiation therapy techniques. In: Bruinvis IAD, van der Giessen PH, van Klessens HJ, *et al.*, editors. The use of computers in radiation therapy. North Holland, The Netherlands: Elsevier; 1987. p. 227–230.
  58. Brahme A, Ågren A. Optimal dose distribution for eradication of heterogeneous tumors. *Acta Oncol* 1987;26:377–385.
  59. Cormack A. A problem in rotation therapy with x-rays. *Int J Radiat Oncol Biol Phys* 1987;13:623–630.
  60. Cormack AM, Cormack RA. A problem in rotation therapy with x-rays: Dose distributions with an axis of symmetry. *Int J Radiat Oncol Biol Phys* 1987;13:1921–1925.
  61. Brahme A, Kraepelien T, Svensson H. Electron and photon beams from a 50 MeV racetrack microtron. *Acta Radiol Oncol* 1980;19:305–319.
  62. Brahme A, Reisdorf D. Microtrons for electron and photon radiotherapy. *IEEE Trans Nucl Sci* 1981;NS-28:1880–1883.
  63. Nafstad P, Brahme A, Nordell B. Computer assisted dosimetry of scanned electron and photon beams for radiation therapy. *Radiother Oncol* 1984;2:261–269.
  64. Kallman P, Lind B, Eklof A, *et al.* Shaping of arbitrary dose distributions by dynamic multileaf collimation. *Phys Med Biol* 1988;33:1291–1300.
  65. Lind B, Kallman P. Experimental verification of a new inversion algorithm for radiation therapy planning. *Radiother Oncol* 1990;17:359–368.
  66. Bortfeld T, Burkelbach J, Boesecke R, *et al.* Methods of image reconstruction from projections applied to conformation radiotherapy. *Phys Med Biol* 1990;35:1423–1434.
  67. Karlsson MG, Karlsson M, Zackrisson B. Intensity modulation with electrons: Calculations, measurements and clinical applications. *Phys Med Biol* 1998;43:1159–1169.
  68. Lief EP, Larsson A, Humm JL. Electron dose profile shaping by modulation of a scanning elementary beam. *Med Phys* 1996;23:33–34.
  69. Lief EP, Lo YC, Humm JL. Electron wedges for radiation therapy. *Int J Radiat Oncol Biol Phys* 1998;40:233–243.
  70. Mackie TR, Holmes T, Swerdloff S, *et al.* Tomotherapy: A new concept for the delivery of dynamic conformal radiotherapy. *Med Phys* 1993;20:1709–1719.
  71. Carol MP. Integrated 3-D conformal multivane intensity modulation delivery system for radiotherapy. Proceedings of the 11th International Conference on the Use of Computers in Radiation Therapy, Madison, WI, 1994.
  72. Carol MP. Integrated 3D conformal planning/multivane intensity modulating delivery system for radiotherapy. In: Purdy JA, Emami B, editors. 3D radiation treatment planning and conformal therapy. Madison, WI: Medical Physics Publishing; 1995. p. 435–445.
  73. Sultanem J, Shu HK, Xia P, *et al.* Three-dimensional intensity-modulated radiotherapy in the treatment of nasopharyngeal carcinoma: The University of California–San Francisco experience. *Int J Radiat Oncol Biol Phys* 2000;48:711–722.
  74. Carol M, Grant W IIIH, Bleier AR, *et al.* The field-matching problem as it applies to the Peacock three-dimensional conformal system for intensity modulation. *Int J Radiat Oncol Biol Phys* 1996;34:183–187.
  75. Low DA, Mutic S. Abutment region dosimetry for sequential arc IMRT delivery. *Phys Med Biol* 1997;42:1465–1470.
  76. Mackie TR. Tomotherapy. Proceedings of the XII International Conference on the Use of Computers in Radiation Therapy, Salt Lake City, Utah. 1997.
  77. Ruchala KJ, Olivera GH, Schloesser EA, *et al.* Megavoltage CT on a tomotherapy system. *Phys Med Biol* 1999;44:2597–2621.
  78. Convery DJ, Rosenbloom ME. The generation of intensity-modulated fields for conformal radiotherapy by dynamic collimation. *Phys Med Biol* 1992;37:1359–1374.
  79. Bortfeld T, Boyer AL, Schlegel W, *et al.* Realization and verification of the three dimensional conformal radiotherapy with modulated fields. *Int J Radiat Oncol Biol Phys* 1994;30:899–908.
  80. Spirou SV, Chui CS. Generation of arbitrary intensity profiles by dynamic jaws or multileaf collimators. *Med Phys* 1994;21:1031–1041.
  81. Dirks MLP, Heijmen BJM, Santvoort JPC. Leaf trajectory calculation for dynamic multileaf collimation to realize optimized fluence profiles. *Phys Med Biol* 1998;43:1171–1184.
  82. Bortfeld T, Kahler DL, Waldron TJ, *et al.* X-ray field compensation with multileaf collimators. *Int J Radiat Oncol Biol Phys* 1994;28:723–730.
  83. Siochi RAC. Minimizing static intensity modulation delivery time using an intensity solid paradigm. *Int J Radiat Oncol Biol Phys* 1999;43:671–680.
  84. Yu CX. Intensity modulated arc therapy with dynamic multileaf collimation: An alternative to tomotherapy. *Phys Med Biol* 1995;40:1435–1449.
  85. Yu C, Symons MJ, Du MN, *et al.* A method for implementing dynamic photon beam intensity modulation using independent jaws and a multileaf collimator. *Phys Med Biol* 1995;40:769–787.
  86. Yu CX. Intensity modulated arc therapy: A new method for delivering conformal radiation therapy. In: Sternick ES, editor. The theory & practice of intensity modulated radiation therapy. Madison, WI: Advanced Medical Publishing; 1997. p. 107–120.
  87. Yu CX, Chen DJ, Li A, *et al.* Intensity-modulated arc therapy: Clinical implementation and experience. Proceedings of

- the XIIIth International Conference on the Use of Computers in Radiotherapy, Heidelberg, Germany, 2000.
88. Gustafsson A, Lind BK, Svensson R, *et al.* Simultaneous optimization of dynamic multileaf collimation and scanning patterns or compensation filters using a generalized pencil beam algorithm. *Med Phys* 1995;22:1141–1156.
  89. Stein J, Hartwig K, Levegrün S, *et al.* Intensity-modulated treatments: Compensators vs. multileaf modulation. Proceedings of the XII International Conference on the Use of Computers in Radiation Therapy, Salt Lake City, UT, 1997.
  90. Mageras GS, Mohan R, Burman C, *et al.* Compensators for three-dimensional treatment planning. *Med Phys* 1991;18:133–140.
  91. Jiang SB, Ayyangar KM. On compensator design for photon beam intensity-modulated conformal therapy. *Med Phys* 1998;25:668–675.
  92. Basran PS, Ansbacher W, Field CG, *et al.* Evaluation of optimized compensators on a 3D planning system. *Med Phys* 1998;25:1837–1844.
  93. Chang SX, Deschesne KM, Cullip T, *et al.* A comparison of different intensity modulation treatment techniques for tangential breast irradiation. *Int J Radiat Oncol Biol Phys* 1999;45:1305–1314.
  94. Dubal N, Chang S, Cullip T, *et al.* Intensity modulation for tangential breast treatment (abstract). *Int J Radiat Oncol Biol Phys* 1998;42:127.
  95. Schweikard A, Tombropoulos R, Adler JR. Robotic radiosurgery with beams of adaptable shapes. In: Ayache N, editor. Computer vision and robotics in medicine. Lecture Notes in Computer Science (LNCS) 905. New York: Springer; 1995. p. 138–149.
  96. Webb S. Conformal intensity-modulated radiotherapy (IMRT) delivered by robotic linac—Testing IMRT to the limit? *Phys Med Biol* 1999;44:1639–1654.
  97. Webb S. Conformal intensity-modulated radiotherapy (IMRT) delivered by robotic linac—Conformality versus efficiency of dose delivery. *Phys Med Biol* 2000;45:1715–1730.
  98. Bortfeld T, Schlegel W. Optimization of beam orientations in radiation therapy: Some theoretical considerations. *Phys Med Biol* 1993;38:291–304.
  99. Brahme A. Optimization of stationary and moving beam radiation therapy techniques. *Radiation Oncol* 1988;12:129–140.
  100. Webb S. Optimization of conformal radiotherapy dose distributions by simulated annealing. *Phys Med Biol* 1989;34:1349–1370.
  101. Webb S. Optimization by simulated annealing of three-dimensional conformal treatment planning for radiation fields defined by a multileaf collimator. *Phys Med Biol* 1991;36:1201–1226.
  102. Webb S. Optimization of conformal radiotherapy dose distributions by simulated annealing. II. Inclusion of scatter in the 2D technique. *Phys Med Biol* 1991;36:1227–1237.
  103. Webb S. Optimization by simulated annealing of three-dimensional, conformal treatment planning for radiation fields determined by a multileaf collimator. II. Inclusion of two-dimensional modulation of the x-ray intensity. *Phys Med Biol* 1992;37:1689–1704.
  104. Mohan R, Mageras GS, Baldwin B, *et al.* Clinically relevant optimization of 3-D conformal treatments. *Med Phys* 1992;19:933–944.
  105. Mohan R, Wang X, Jackson A, *et al.* The potential and limitations of the inverse radiotherapy technique. *Radiation Oncol* 1994;32:232–248.
  106. Holmes T, Mackie TR. A comparison of three inverse treatment planning algorithms. *Phys Med Biol* 1994;39:91–106.
  107. Bahr GK, Kereiakes JG, Horwitz H. The method of linear programming applied to radiation treatment planning. *Radiology* 1968;91:686–693.
  108. Hodes L. Semiautomatic optimization of external beam radiation treatment planning. *Radiology* 1974;110:191–196.
  109. Hope CS, Laurie J, Orr JS, *et al.* Optimization of x-ray treatment planning by computer judgment. *Phys Med Biol* 1967;12:531–542.
  110. McDonald SC, Rubin P. Optimization of external beam radiation therapy. *Int J Radiat Oncol Biol Phys* 1977;2:307–317.
  111. Morrill SM, Lane RG, Jacobson G, *et al.* Treatment planning optimization using constrained simulated annealing. *Phys Med Biol* 1991;36:1341–1361.
  112. Powlis WD, Altschuler MD, Censor Y, *et al.* Semi-automated radiotherapy treatment planning with a mathematical model to satisfy treatment goals. *Int J Radiat Oncol Biol Phys* 1989;16:271–276.
  113. Rosen II, Lane RG, Morrill SM, *et al.* Treatment plan optimization using linear programming. *Med Phys* 1991;18:141–152.
  114. Starkschall G. A constrained least-squares optimization method for external beam radiation therapy treatment planning. *Med Phys* 1984;11:659–665.
  115. Mohan R, Wang X, Jackson A. Optimization of 3-D conformal radiation treatment plans. In: Meyer JL, Purdy JA, editors. Frontiers of radiation therapy and oncology. 3-D conformal radiotherapy: A new era in the irradiation of cancer. Basel: Karger; 1996. p. 86–103.
  116. Jackson A, Kutcher GJ. Probability of radiation-induced complication for normal tissues with parallel architecture subject to non-uniform irradiation. *Med Phys* 1993;20:613–625.
  117. Kallman P, Lind B, Brahme A. An algorithm for maximizing the probability of complication-free tumor control in radiation therapy. *Phys Med Biol* 1992;37:871–890.
  118. Niemierko A, Goitein M. Calculation of normal tissue complication probability and dose-volume histogram reduction schemes for tissues with a critical element architecture. *Radiation Oncol* 1991;20:166–176.
  119. Niemierko A, Urie M, Goitein M. Optimization of 3D radiation therapy with both physical and biological end points and constraints. *Int J Radiat Oncol Biol Phys* 1992;23:99–108.
  120. Niemierko A, Goitein M. Modeling of normal tissue response to radiation: The critical volume model. *Int J Radiat Oncol Biol Phys* 1992;25:135–145.
  121. Niemierko A, Goitein M. Implementation of a model for estimating tumor control probability for an inhomogeneously irradiated tumor. *Radiation Oncol* 1993;29:140–147.
  122. Niemierko A. Reporting and analyzing dose distributions: A concept of equivalent uniform dose. *Med Phys* 1997;24:103–110.
  123. Kessler ML, Kim JJH, McShan DL, *et al.* A general framework for interactive and automated treatment plan optimization. Part I: Evaluators, modifiers, and costlets (abstract). *Med Phys* 1998;25:A178.
  124. Brahme A, Roos JE, Lax I. Solution of an integral equation encountered in rotation therapy. *Phys Med Biol* 1982;27:1221–1229.
  125. Bortfeld T. Optimized planning using physical objectives and constraints. *Semin Radiation Oncol* 1999;9:20–34.
  126. Spirou SV, Chui CS. A gradient inverse planning algorithm with dose-volume constraints. *Med Phys* 1998;25:321–333.
  127. Xing L, Chen GTY. Iterative algorithms for inverse treatment planning. *Phys Med Biol* 1996;41:2107–2123.
  128. Xing L, Li JG, Pugachev A, *et al.* Estimation theory and model parameter selection for therapeutic treatment plan optimization. *Med Phys* 1999;26:2348–2358.

129. Mageras GS, Mohan R. Application of fast simulated annealing to optimization of conformal radiation treatments. *Med Phys* 1993;20:639–647.
130. Stein J, Mohan R, Wang X-H, *et al.* Optimum number and orientations of beams for intensity-modulated treatments (abstract). *Med Phys* 1996;23:1063.
131. Deasy JO. Multiple local minima in radiotherapy optimization problems with dose-volume constraints. *Med Phys* 1997;24:1157–1161.
132. Ezzell GA. Genetic and geometric optimization of three-dimensional radiation therapy. *Med Phys* 1996;23:293–305.
133. Galvin JM, Xuan-Gen C, Smith RM. Combining multileaf fields to modulate fluence distributions. *Int J Radiat Oncol Biol Phys* 1993;27:697–705.
134. Boyer AL, Yu CX. Intensity modulated radiation therapy with dynamic multileaf collimators. *Semin Radiat Oncol* 1999;9:48–59.
135. Van Santvoort JPC, Heijmen BJM. Dynamic multileaf collimation without “tongue-and-groove” underdosage effects. *Phys Med Biol* 1996;41:2091–2105.
136. Webb S, Bortfeld T, Stein J, *et al.* The effect of stair-step leaf transmission on the “tongue-and-groove” problem in dynamic radiotherapy with a multileaf collimator. *Phys Med Biol* 1997;42:595–602.
137. Mackie TR, Reckwerdt P, McNutt T, *et al.* Photon beam dose computations. In: Palta J, Mackie TR, editors. *Teletherapy: Present and future*. College Park, MD: Advanced Medical Publishing; 1996. p. 103–136.
138. Ahnesjö A, Aspradakis MM. Dose calculations for external photon beams in radiotherapy. *Phys Med Biol* 1999;44:R99–R155.
139. Bourland JD, Chaney EL. A finite-size pencil beam model for photon dose calculations in three dimensions. *Med Phys* 1992;19:1401–1412.
140. Ostapiak OZ, Zhu Y, Van Dyk J. Refinements of the finite-size pencil beam model of three-dimensional photon dose calculation. *Med Phys* 1997;24:743–750.
141. Mackie TR, Scrimger JW, Battista JJ. A convolution method of calculating dose for 15-MV x-rays. *Med Phys* 1985;12:188–196.
142. Boyer A, Mok E. A photon dose distribution model employing convolution methods. *Med Phys* 1985;12:169–177.
143. Ahnesjö A. Collapsed cone convolution of radiant energy for photon dose calculation in heterogeneous media. *Med Phys* 1989;16:577–592.
144. Battista JJ, Sharpe MB. True three-dimensional dose computations for megavoltage x-ray therapy: A role for the superposition principle. *Aust Phys Eng Sci Med* 1992;15:159–178.
145. Mohan R, Chui C, Lidofsky L. Differential pencil beam dose computation model for photons. *Med Phys* 1986;13:64–73.
146. Chui CS, LoSasso T, Spirou S. Dose calculations for photon beams with intensity modulation generated by dynamic jaw or multi-leaf collimations. *Med Phys* 1994;21:1237–1243.
147. Mackie TR, El-Khatib E, Battista JJ, *et al.* Lung corrections for 6- and 15-MV x-rays. *Med Phys* 1985;12:327–332.
148. Wong JW, Purdy JA. On methods of inhomogeneity corrections for photon transport. *Med Phys* 1990;17:807–814.
149. McShan D, Fraass B, Kessler M. Intensity modulation using beamlets (abstract). *Med Phys* 1998;25:A149.
150. Hartmann Siantar CL, Bergstrom PM, Chandler WP, *et al.* Lawrence Livermore National Laboratory’s PEREGRINE Project. Proceedings of the XII International Conference on the Use of Computers in Radiation Therapy, Salt Lake City, Utah, 1997.
151. Ma C-M, Mok E, Kapur A, *et al.* Clinical implementation of a Monte Carlo treatment planning system. *Med Phys* 1999;26:2133–2143.
152. Schach von Wittenau AE, Cox LJ, Bergstrom PM, *et al.* Correlated histogram representation of Monte Carlo derived medical accelerator photon-output phase space. *Med Phys* 1999;26:1196–1211.
153. Sempau J, Wilderman SJ, Bielajew AF. DPM, a fast, accurate Monte Carlo code optimized for photon and electron radiotherapy treatment planning dose calculations. *Phys Med Biol* 2000;45:2263–2291.
154. Woo MK, Cunningham JR, Jerioranski JJ. Extending the concept of primary and scatter separation to the condition of electronic disequilibrium. *Med Phys* 1990;17:588–595.
155. Jaffray DA, Battista JJ, Fenster A, *et al.* X-ray sources of medical linear accelerators: Focal and extra-focal radiation. *Med Phys* 1993;20:1417–1427.
156. Chen Y, Boyer A, Ma CM. Calculation of x-ray transmission through a multileaf collimator. *Med Phys* 2000;27:1717–1726.
157. Mackie TR. Applications of the Monte Carlo method in radiotherapy. In: Kase KR, Bjarngard BE, Attix FH, editors. *The dosimetry of ionizing radiation*. Vol. III. San Diego: Academic Press; 1990.
158. Boyer A, Xing L, Ma C-M, *et al.* Theoretical considerations of monitor unit calculations for intensity modulated beam treatment planning. *Med Phys* 1999;26:187–195.
159. Mackie TR, Reckwerdt P, Papanikolaou N. 3-D photon beam dose algorithms. In: Purdy JA, Emami B, editors. *3D radiation treatment planning and conformal therapy*. Madison, WI: Medical Physics Publishing; 1995. p. 201–222.
160. Ahnesjö A. Application of the convolution method for calculation of output factors for therapy photon beams. *Med Phys* 1992;19:295–301.
161. Ahnesjö A. Analytic modeling of photon scatter from flattening filters in photon therapy beams. *Med Phys* 1994;21:295–301.
162. Ahnesjö A. Collimator scatter in photon therapy beams. *Med Phys* 1995;22:267–278.
163. Liu H, Mackie TR, McCullough EC. A dual source photon beam model used in convolution/superposition dose calculation for clinical megavoltage x-ray beam. *Med Phys* 1997;24:1960–1974.
164. Fraass B, Doppke K, Hunt M, *et al.*, for the AAPM Radiation Therapy Committee Task Group 53. Quality assurance for clinical radiotherapy treatment planning. *Med Phys* 1998;25:1773–1829.
165. Van Dyk J, Barrett RB, Cygler JE, *et al.* Commissioning and quality assurance of treatment planning computers. *Int J Radiat Oncol Biol Phys* 1993;26:261–273.
166. Fraass BA, Martel MK, McShan DL. Tools for dose calculation verification and QA for conformal therapy treatment techniques. Proceedings of the XIth International Conference on the Use of Computers in Radiation Therapy, Manchester, UK, 1994.
167. Harms WB Sr, Low DA, Wong JW, *et al.* A software tool for the quantitative evaluation of 3D dose calculation algorithms. *Med Phys* 1998;25:1830–1836.
168. Low DA, Mutic S, Harms WB Sr, *et al.* A technique for the quantitative evaluation of dose distributions. *Med Phys* 1998;25:656–661.
169. Ezzell GA, Schild SE, Wong WW. Development of a treatment planning protocol for prostate treatments using intensity modulated radiotherapy. *J Appl Clin Med Phys* 2001;2:59–68.
170. Low DA, Mutic S, Gerber RL, *et al.* Quantitative dosimetric verification of an IMRT planning and delivery system. *Radiation Oncol* 1999;49:305–316.
171. Maryanski MJ, Ibbott GS, Eastman P, *et al.* Radiation therapy dosimetry using magnetic resonance imaging of polymer gels. *Med Phys* 1996;23:699–705.

172. Kelly R, Jordan K, Battista J. Optical CT reconstruction of 3D dose distributions using the ferrous-benzoic-xyleneol (FBX) gel dosimeter. *Med Phys* 1998;25:1741–1750.
173. Maryanski MJ, Zastavker YZ, Gore JC. Radiation dose distributions in three dimensions from tomographic optical density scanning of polymer gels: II. Optical properties of the BANG polymer gel. *Phys Med Biol* 1996;41:2705–2717.
174. Ma CM, Pawlicki T, Jiang SB, *et al.* Monte Carlo verification of IMRT dose distributions from a commercial treatment planning optimization system. *Phys Med Biol* 2000;45:2483–2495.
175. Xing L, Curran B, Hill R, *et al.* Dosimetric verification of a commercial inverse treatment planning system. *Phys Med Biol* 1999;44:463–478.
176. Xing L, Chey Y, Luxton G, *et al.* Monitor unit calculation for intensity modulated photon field by a simple scatter-summation algorithm. *Phys Med Biol* 2000;45:N1–N7.
177. Geis PG, Boyer AL, Wells NH. Use of a multileaf collimator as a dynamic missing tissue compensator. *Med Phys* 1996; 23:1199–1205.
178. Kung JH, Chen GTY, Kuchnir FK. A monitor unit verification calculation in intensity modulated radiotherapy as a dosimetry quality assurance. *Med Phys* 2000;27:2226–2230.
179. Purdy JA, Biggs PJ, Bowers C, *et al.* Medical accelerator safety considerations. Report of AAPM Radiation Therapy Committee Task Group No. 35. *Med Phys* 1993;20:1261–1275.
180. Kutcher GJ, Coia L, Gillin M, *et al.* Comprehensive QA for radiation oncology. Report of AAPM Radiation Therapy Committee Task Group 40. *Med Phys* 1994;21:581–618.
181. Low DA, Mutic S, Dempsey JF, *et al.* Abutment dosimetry for serial tomotherapy. *Med Dosim* 2001;26:79–81.
182. LoSasso T, Chiu CS, Ling CC. Physical and dosimetric aspects of a multileaf collimation system used in the dynamic mode for implementing intensity modulated radiotherapy. *Med Phys* 1998;25:1919–1927.
183. Low DA, Zhu XR, Purdy JA, *et al.* The influence of angular misalignment on fixed-portal intensity modulated radiation therapy. *Med Phys* 1997;24:1123–1139.
184. Chui CS, Spirou S, LoSasso T. Testing of dynamic multileaf collimation. *Med Phys* 1996;23:635–641.
185. Partridge M, Evans PM, Mosleh-Shirazi A, *et al.* Independent verification using portal imaging of intensity-modulated beam delivery by the dynamic MLC technique. *Med Phys* 1998;25:1872–1881.
186. Keller H, Fix MK, Liistro L, *et al.* Theoretical considerations to the verification of dynamic multileaf collimated fields with a SLIC-type portal image detector. *Phys Med Biol* 2000;45: 2531–2545.
187. Burman C, Chui CS, Kutcher G, *et al.* Planning, delivery, and quality assurance of intensity-modulated radiotherapy using dynamic multileaf collimator: A strategy for large-scale implementation for the treatment of carcinoma of the prostate. *Int J Radiat Oncol Biol Phys* 1997;39:863–873.
188. National Council on Radiation Protection and Measurements. Structural shielding design and evaluation for medical use of x rays and gamma rays of energies up to 10 MeV. Washington, DC: NCRP; 1976.
189. National Council on Radiation Protection and Measurements. Radiation protection design guidelines for 0.1–100 MeV particle accelerator facilities. Washington, DC: NCRP; 1977.
190. Followill D, Geis P, Boyer A. Estimates of whole-body dose equivalent produced by beam intensity modulated conformal therapy. *Int J Radiat Oncol Biol Phys* 1997;38:667–672.
191. Followill D, Geis P, Boyer A. Errata: Estimates of whole-body dose equivalent produced by beam intensity modulated conformal therapy. *Int J Radiat Oncol Biol Phys* 1997;38: 783.
192. Grant W III. Private communication. 1999.
193. Mutic S, Low DA. Whole-body dose from tomotherapy delivery. *Int J Radiat Oncol Biol Phys* 1998;42:229–232.
194. Grant W III, Bleier A, Campbell C, *et al.* Leakage considerations with a multi-leaf collimator designed intensity-modulated conformal radiotherapy (abstract). *Med Phys* 1994;21: 921.
195. Dutriex A. Prescription, precision and decision in treatment planning. *Int J Radiat Oncol Biol Phys* 1987;13:1291–1296.
196. Hendrickson F. Dose prescription dilemma (editorial). *Int J Radiat Oncol Biol Phys* 1988;14:595–596.
197. International Commission on Radiation Units and Measurements. Dose specification for reporting external beam therapy with photons and electrons. Washington, DC: ICRU; 1978.
198. International Commission on Radiation Units and Measurements. Prescribing, recording, and reporting photon beam therapy. Bethesda: ICRU; 1993.
199. International Commission on Radiation Units and Measurements. Prescribing, recording, and reporting photon beam therapy (supplement to ICRU Report 50). Bethesda: ICRU; 1999.
200. Ten Haken RK, Thornton AF, Sandler HM, *et al.* A quantitative assessment of the addition of MRI to CT-based, 3-D treatment planning of brain tumors. *Radiation Oncol* 1992; 25:121–133.
201. Austin-Seymour M, Chen GTY, Rosenman J, *et al.* Tumor and target delineation: Current research and future challenges. *Int J Radiat Oncol Biol Phys* 1995;33:1041–1052.
202. Balter J, Ten Haken R, Lam K. Immobilization and setup verification. In: Palta J, Mackie TR, editors. Teletherapy: Present and future. College Park, MD: Advanced Medical Publishing; 1996. p. 471–494.
203. Langen KM, Jones DTL. Organ motion and its management. *Int J Radiat Oncol Biol Phys* 2001;50:265–278.
204. Jaffray DA, Yan D, Wong JW. Managing geometric uncertainty in conformal intensity modulated radiation therapy. *Semin Radiat Oncol* 1999;9:4–19.
205. Yan D, Ziaga E, Jaffray D. The use of adaptive radiation therapy to reduce setup error: A prospective clinical study. *Int J Radiat Oncol Biol Phys* 1998;41:715–720.
206. Balter JM, Lam K, Sandler HM, *et al.* Measurement of prostate movement over the course of routine radiotherapy using implanted markers. *Int J Radiat Oncol Biol Phys* 1995;31:113–118.
207. Lattanzi J, McNeeley S, Pinover W, *et al.* A comparison of daily CT localization to a daily ultrasound-based system in prostate cancer. *Int J Radiat Oncol Biol Phys* 1999;43:719–725.
208. van Herk M, Bruce A, Kroes APG, *et al.* Quantification of organ motion during conformal radiotherapy of the prostate by three dimensional image registration. *Int J Radiat Oncol Biol Phys* 1995;33:1311–1320.
209. Teh BS, Mai WY, Uhl BM, *et al.* Intensity-modulated radiation therapy (IMRT) for prostate cancer with the use of a rectal balloon for prostate immobilization: Acute toxicity and dose–volume analysis. *Int J Radiat Oncol Biol Phys* 2001; 49:705–712.
210. Ten Haken RK, Balter JM, Marsh LH, *et al.* Potential benefits of eliminating planning target volume expansions for patient breathing in the treatment of liver tumors. *Int J Radiat Oncol Biol Phys* 1997;38:613–617.
211. Kubo HD, Wang L. Compatibility of Varian 2100C gated operations with enhanced dynamic wedge and IMRT dose delivery. *Med Phys* 2000;27:1732–1737.
212. Rosenzweig KE, Hanley J, Mah D, *et al.* The deep inspira-

- tion breath-hold technique in the treatment of inoperable non-small-cell lung cancer. *Int J Radiat Oncol Biol Phys* 2000;48:81–87.
213. Wong J, Sharpe M, Jaffray D. The use of active breathing control (ABC) to minimize breathing motion in conformal therapy. In: Leavitt DD, Starkschall G, editors. Proceedings of the XIIIth International Conference on the Use of Computers in Radiation Therapy. Madison, WI: Medical Physics Publishing; 1997. p. 220–222.
  214. Aaltonen P, Brahme A, Lax I, *et al.* Specification of dose delivery in radiation therapy: Recommendations by the Nordic Association of Clinical Physics (NACP). *Acta Oncol* 1997;36(Suppl. 10):1–32.
  215. McGary JE, Grant W, Woo SY, *et al.* Comment on “Reporting and analyzing dose distributions: A concept of equivalent uniform dose” [Med Phys 1997;24:103–109]. *Med Phys* 1997;24:1323–1324.
  216. Niemierko A. Response to “Comment on ‘Reporting and analyzing dose distributions: A concept of equivalent uniform dose’” [Med Phys 1997;24:1323–1324]. *Med Phys* 1997;24:1325–1327.
  217. Verhey LJ. Comparison of three-dimensional conformal radiation therapy and intensity-modulated radiation therapy systems. *Semin Radiat Oncol* 1999;9:78–98.
  218. Lomax AJ, Bortfeld T, Goitein G, *et al.* A treatment planning inter-comparison of proton and intensity modulated photon radiotherapy. *Radiother Oncol* 1999;51:257–271.
  219. Hong L, Hunt M, Chui C, *et al.* Intensity-modulated tangential beam irradiation of the intact breast. *Int J Radiat Oncol Biol Phys* 1999;44:1155–1164.
  220. Pickett B, Vigneault E, Kurhanewicz J, *et al.* Static field intensity modulation to treat a dominant intra-prostatic lesion to 90 Gy compared to seven field 3-dimensional radiotherapy. *Int J Radiat Oncol Biol Phys* 1999;43:921–929.
  221. Shu H-KG, Lee TT, Vigneault E, *et al.* Toxicity following high-dose three-dimensional conformal and intensity modulated radiation therapy for clinically localized prostate cancer. *Urology* 2001;57:102–107.
  222. Khoo VS, Oldham M, Adams EJ, *et al.* Comparison of intensity-modulated tomotherapy with stereotactically guided conformal radiotherapy for brain tumors. *Int J Radiat Oncol Biol Phys* 1999;45:415–425.
  223. Cardinale RM, Benedict SH, Wu Q, *et al.* A comparison of three stereotactic radiotherapy techniques: ARCS vs. noncoplanar fixed fields vs. intensity modulation. *Int J Radiat Oncol Biol Phys* 1998;42:431–436.
  224. Tsai JS, Engler MJ, Ling MN, *et al.* A non-invasive immobilization system and related quality assurance for dynamic intensity modulated radiation therapy of intracranial and head and neck disease. *Int J Radiat Oncol Biol Phys* 1999;43:455–467.
  225. Verellen D, Linthout N, Storme G. Target localization and treatment verification for intensity modulated conformal radiation therapy of the head and neck region. The AZ-VUB experience. *Strahlenther Onkol* 1998;174:19–27.
  226. De Neve W, De Gerssem W, Derycke S, *et al.* Clinical delivery of intensity modulated conformal radiotherapy for relapsed or second-primary head and neck cancer using a multileaf collimator with dynamic control. *Radiother Oncol* 1999;50:301–314.
  227. Eisbruch A, Marsh LH, Martel MK, *et al.* Comprehensive irradiation of head and neck cancer using conformal multi-segmental fields: assessment of target coverage and noninvolved tissue sparing. *Int J Radiat Oncol Biol Phys* 1998;41:559–568.
  228. Kuppersmith RB, Greco SC, Teh BS, *et al.* Intensity-modulated radiotherapy: First results with this new technology on neoplasms of the head and neck. *Ear Nose Throat* 1999;78:241–246.
  229. Butler EB, Teh BS, Grant WH, *et al.* SMART (simultaneous modulated accelerated radiation therapy) boost: A new accelerated fractionation schedule for the treatment of head and neck cancer with intensity modulated radiotherapy. *Int J Radiat Oncol Biol Phys* 1999;45:21–32.
  230. Grant W III, Cain RB. Intensity modulated conformal therapy for intracranial lesions. *Med Dosim* 1998;23:237–241.
  231. Damen EMF, Brugmans MJP, van der Horst A, *et al.* Planning, computer optimization, and dosimetric verification of a segmented irradiation technique for prostate cancer. *Int J Radiat Oncol Biol Phys* 2001;49:1183–1195.
  232. Lichter AS. Three-dimensional conformal radiation therapy: A testable hypothesis. *Int J Radiat Oncol Biol Phys* 1991;21:853–855.

## APPENDIX

### IMRT nomenclature

**Beamlet (also referred to as a ray or bixel):** A small photon intensity element used to subdivide an intensity-modulated beam for the purposes of intensity distribution optimization or dose calculation. Intensity is defined as fluence or energy fluence, depending on the dose-calculation algorithm used.

**Class solution:** This term refers to the historical experience in designing RT plans for a particular site. Examples include breast tangents, 3-field head-and-neck plans, 4-field pelvic plans, and so forth. Class solutions are often the starting point for optimized forward treatment planning. An IMRT class solution for a given treatment site and stage of disease consists of the criteria for optimization (the form of the objective function and values of its parameters) and the specification of the beam techniques used, typically including beam directions and number. Once developed, a class solution may be applied repeat-

edly to generate IMRT plans for patients with the same stage of disease at the same site and for other similar clinical considerations.

**Dynamic multileaf collimator (DMLC)–IMRT:** A method used to deliver intensity-modulated beams using an MLC, with the leaves in motion during radiation delivery. The *sliding window* technique is a form of DMLC–IMRT in which the window formed by each opposing pair of leaves traverses across the tumor volume while the beam is on.

**Field:** Dose delivered from one beam direction; can be a flat-intensity profile (normal flat field) or a non-uniform fluence distribution delivered with multiple static MLC segments (SMLC) or DMLC techniques.

**Forward planning:** Treatment planning in which the planner defines the beam directions and shapes, beam weights, wedges, blocks, margins, and so on, followed by the dose calculation and then the display and evaluation of the dose

distribution. Iteration through the process is performed manually to reach an optimal (or at least an acceptable) plan.

**Intensity-modulated radiotherapy (IMRT):** An advanced form of 3D-CRT that uses non-uniform radiation beam intensities incident on the patient that have been determined using various computer-based optimization techniques.

**Inverse planning:** Treatment planning in which the clinical objectives are specified mathematically and a computer optimization algorithm is used to automatically determine beam parameters (mainly beamlet weights) that will lead to the desired dose distribution. Inverse planning is sometimes confused with matrix inversion of a given dose distribution, although this is not actually how any current inverse planning system works.

**Objective function (cost function):** A mathematical description of criteria of treatment plan optimization (i.e., clinical objectives). Optimization criteria may be specified in terms of dose-limits, dose-volume limits, dose-response functions (TCP, NTCPs, etc.), or other formulations.

**Score (cost):** The numerical value of the objective function that represents a figure of merit indicating the quality of the treatment plan. The best plan corresponds to the extremum score. The extremum may be a minimum or a maximum depending on the way the objective function is defined.

**Segment:** Shaped aperture with uniform fluence; typically one of many MLC shapes that have the same beam direction that is used to create an intensity-modulated field.

**Segmental multileaf collimator (SMLC)-IMRT:** An automated method to deliver an intensity modulated beam at a fixed beam direction with a sequence of MLC segments in which the radiation is turned on only when the MLC leafs come to a stop at each prescribed segment position. The term SMLC-IMRT should replace *step-and-shoot*, *stop-and-shoot*, *move-and-shoot*, and other similar permutations used for this type of IMRT.

**Three-dimensional conformal radiotherapy (3D-CRT):** An advanced form of external beam RT in which the high-dose treated volume is planned to encompass the 3D target volume (cancerous cells), at the same time minimizing the dose to the surrounding organs at risk. It requires 3D treatment planning and is typically accomplished with a set of fixed radiation beams, which are shaped using the projection of the target. The radiation beams typically have a uniform intensity across the field, or, where appropriate, have this intensity modified by simple beam-modifying devices like wedges or compensating filters. Referred to as conventional 3D-CRT in this document.

**Tomotherapy:** The delivery of intensity modulated rotating fan beams. *Serial tomotherapy* is the delivery of multiple fan beams with discrete table increments between each axial gantry arc. *Helical tomotherapy* makes use of helical CT type motions (continuous synchronized gantry and table motion).